Conformations of Amatoxins in the Crystalline State

G. Shoham,*,† W. N. Lipscomb,‡ and Th. Wieland§

Contribution from the Department of Inorganic and Analytical Chemistry, The Hebrew University of Jerusalem, Jerusalem 91904, Israel, Gibbs Laboratory, Department of Chemistry, Harvard University, Cambridge, Massachusetts 02138, and the Max Planck Institute for Medical Research, Heidelberg, Germany. *Received August 24, 1987*

Abstract: The amatoxins consist of a family of bicyclic octapeptides present in the poisonous mushroom *Amanita phalloides* and their synthetic derivatives. The crystal structures of the slightly toxic (*S*)-sulfoxide isomer of *o*-methyl-α-amanitin (**7**) and the highly toxic *O*-methyl-*S*-oxo-α-amanitin (**8**) have been determined by single-crystal X-ray diffraction techniques. The structures were solved by direct methods and refined by least-squares procedures to final *R* factors of 0.063 and 0.068 for **7** and **8**, respectively. Both crystals display the symmetry of the orthorhombic space group $P2_12_12_1$ with 4 formula units in the unit cell. Unit cell dimensions of **7** are a = 15.883 Å, b = 18.245 Å, and c = 20.247 Å, and there are 6 methanol molecules and a water molecule in each crystallographic asymmetric unit. Unit cell dimensions of **8** are a = 16.123 Å, b = 18.358 Å, and c = 20.119 Å, and there are 3 ethanol molecules and 4 water molecules in each asymmetric unit. The conformations of amatoxins **7** and **8** are very rigid and they are almost identical. The distorted "T" shape conformation is dominated by five rather strong intramolecular hydrogen bonds: 2 backbone (5→1 and 4→1) hydrogen bonds and 3 backbone/side chain hydrogen bonds. The solvent molecules in both crystals form continuous "channels" along the crystal *b* axis and participate in extensive hydrogen bond networks with the peptides. The structure and conformation of **7** and **8** are similar, for the most part, with those of the toxic β-amanitin (**2**) and the nontoxic *S*-deoxo-Ile^3-amaninamide (**10**), in the crystalline state. Nevertheless, the backbones of **2** and **10** are significantly more similar to each other than to **7** and **8**, primarily due to a 90° rotation of the plane of the peptide bond between Cys-8 and Asn-1 which occurs only in **7** and **8**. There are a few more local conformational differences between the four amatoxin derivatives, but they do not seem to be of functional importance. The structure–activity relationships in the amatoxin series are discussed, mainly on a 3-dimensional structural basis, and it is suggested that most of the differences in the biological activities of amatoxins result from differences in the chemical structure and not from differences in the conformations.

The green death cup *Amanita phalloides* is one of the most toxic plants known.[1-3] The *Amanita* mushrooms are found mainly in Central Europe;[2] however, several species of this family were observed recently in North America.[4,5a] It is believed that 90–95% of all deaths from mushroom poisoning (in Central Europe and North America) can be attributed to *A. phalloides*.[1,2] Of the several oligopeptides produced by *Amanita* mushrooms, three classes are toxic: the amatoxins (octapeptides), the phallotoxins (heptapeptides), and the virotoxins (heptapeptides).[6] All three classes consist of cyclic peptides that contain unusual hydroxylated amino acids. In the amatoxin and the phallotoxin classes the primary cyclopeptide ring is spanned by a sulfur-containing bridge, resulting in a nearly rigid bicyclic frame; the virotoxins, in turn, are monocyclic. The phallotoxins act relatively quickly (death of mice or rats, when injected intravenously or generally by any intraperitoneal injection, occurs within 1 or 2 h, LD_{50} of 1.5–2.5 mg/kg in mice).[7] The phallotoxins bind strongly to F-actin (affinity constant of 10^{-7}–10^{-8} M),[8] especially in liver cells, resulting in high stability of the conjugate against depolymerization and degradation.[6]

The recently discovered virotoxins[9] (observed only in *A. virosa*) are somewhat related to the phallotoxins in chemical structure and are very similar to them in toxicity and biological action. It is likely that the virotoxins are biosynthetically derived from the phallotoxins or from a common precursor molecule.[6]

The amatoxins are slow-acting poisons (lethal interval is at least 15 h) but are, however, 10–20 times more toxic than phallotoxins and virotoxins (LD_{50}'s are in the range of 0.15–0.5 mg/kg in mice).[7] They cause cell necrosis, especially in the liver and the kidneys, leading to death (in humans) in 5–7 days. Since all symptoms described for lethal poisoning with *A. phalloides* mushroom can likewise be produced by pure amatoxins it is concluded that amatoxins are the sole cause of fatal human poisoning.[7]

A typical sample of *A. phalloids* mushroom contains 3–5 mg of amatoxins[5a,b] and 4–6 mg of phallotoxins[7] per gram of dry tissue (or 20 g of fresh tissue); a typical mushroom weights 40–50 g (about 8–12 mg of amatoxins). Since the lethal dose of amatoxins is less than 0.1 mg/kg body weight for humans, it is possible that one mushroom can kill an adult.

The molecular basis of action of amatoxins is the strong inhibition of one of the RNA polymerases, hence blocking an m-RNA synthesis and stopping protein production in affected cells. The amatoxins bind with high affinity ($K_i < 10^{-8}$ M) only to eukaryotic DNA-dependent RNA polymerase B (which transcribes the precursor of m-RNA) and with lower affinity ($K_i > 10^{-5}$ M) to RNA polymerase C.[7] They form a 1:1 complex with either enzyme[10] and bind to the 140 KD subunit (SB3), at least in the case of RNA polymerase B.[11]

Although the molecular mechanism of inhibition is not yet known, it is evident that (a) the toxin forms a quaternary complex with the enzyme, the DNA template, and the produced RNA chain,[10,12] and (b) the toxin does not affect the affinity of RNA polymerase B for any of the 4 nucleotides and does not inhibit the formation of a new phosphodiester bond, but in its presence a subsequent inter-nucleotide bond is not synthesized.[12] It is suggested, therefore, that the translocation of the growing RNA chain to the catalytic site of the enzyme is being blocked.[6,12]

Nine different amatoxins have been isolated from *Amanita* mushroom.[6,7] The general chemical structure of the amatoxins

† The Hebrew University of Jerusalem.
‡ Harvard University.
§ Max Planck Institute for Medical Research.

(1) Wieland, Th. *Science* **1968**, *159*, 946.
(2) Wieland, Th.; ,Wieland, O. In *Microbial Toxins*; Kadis, S., Cigler, A., Ajl, S., Eds.; Academic Press: New York, 1972; Vol. 8, pp 249–280.
(3) Faulstich, H. In *Progress in Molecular and Subcellular Biology*; Hahn, F. E., Ed.; Springer: Berlin, 1980; Vol. 7, pp 88–134.
(4) Tanghe, L. J.; Simons, D. M. *Mycologia* **1973**, *65*, 99.
(5) (a) Yocum, R. R.; Simons, D. M. *Lloydia* **1977**, *40*, 178. (b) Stijve, T.; Diserens, H. In *Amanita Toxins and Poisoning*; Faulstich, H., Kommerell, B., Wieland, Th., Eds.; Witzstrock: Baden-Baden, 1980; pp 30–36.
(6) Wieland, Th. *Int. J. Peptide Protein Res.* **1983**, *22*, 257.
(7) Wieland, Th.; Faulstich, H. *CRC Crit. Rev. Biochem.* **1978**, *5*, 185.
(8) Faulstich, H.; Schäfer, A. J.; Weckauf, M. *Hoppe-Seyler's Z. Physiol. Chem.* **1977**, *358*, 181.
(9) Faulstich, H.; Buku, A.; Bodenmüller, H.; Wieland, Th. *Biochemistry* **1980**, *19*, 3334.
(10) Cochet-Meilhac, M.; Chambon, P. *Biochim. Biophys. Acta* **1974**, *353*, 160.
(11) Brodner, O. G.; Weiland, Th. *Biochemistry* **1976**, *15*, 3480.
(12) Vaisius, A. C.; Wieland, Th. *Biochemistry* **1982**, *21*, 3097.

0002-7863/89/1511-4791$01.50/0

Table I. Chemical Structure, Inhibition Capacity (K_i, 10^{-8} M), and Toxicity (LD_{50}, mg/kg white mouse) of Some Amatoxin Derivatives[a]

no.	name	R^1	R^2	R^3	R^4	R^5	R^6	R^7	X	LD_{50}[c]	K_i
1	α-amanitin	NH_2	OH	$-CH(CH_3)CH(OH)CH_2OH$	OH	H	sBu[b]	H	SO(R)	0.3	0.23
2	β-amanitin	OH	=	=	=	=	=	=	=	0.5	0.25
3	γ-amanitin	=	=	$-CH(CH_3)CH(OH)CH_3$	=	=	=	=	=	0.2	0.5
4	amanullin	=	=	$-CH(CH_3)CH_2CH_3$	=	=	=	=	=	≈15	1.0
5	proamanullin	=	H	$-CH(CH_3)CH_2CH_3$	=	=	=	=	=	>20	5000
6	amaninamide	=	=	=	H	=	=	=	=	≈0.5	≈0.5
7	(*S*)-sulfoxide isomer of 6′-*O*-methyl-α-amanitin	=	=	=	OCH_3	=	=	=	SO(S)	≈15	≈2
8	sulfone-6′-*O*-methyl-*S*-oxo-α-amanitin	=	=	=	OCH_3	=	=	=	SO_2	≈1	0.57
9	6′-*O*-methyl-*S*-deoxo-α-amanitin	=	=	=	OCH_3	=	=	=	S	≈0.5	0.25
10	*S*-deoxo-Ile[3]-amaninamide	=	=	$-CH(CH_3)CH_2CH_3$	H	=	=	=	S	>50	8.1
11	6′-*O*-methylaldoamanitin	=	=	$-CH(CH_3)CHO$	OCH_3	=	=	=	=	>100	100
12	6′-*O*-methyldemethyl-γ-amanitin	=	=	$-CH(CH_3)CH_2OH$	OCH_3	=	=	=	=	3.0	2
13	dinor-*S*-deoxoamaninamide	=	=	$-CH_2CH_2OH$	H	=	=	=	S	>100	5000
14	*S*-deoxo-Ala[3]-amaninamide	=	=	$-CH_3$	H	=	=	=	S		680
15	6′-dehydroxy-*S*-deoxo-Ala[5]-amanullin	=	=	$-CH(CH_3)CH_2CH_3$	H	CH_3	=	=	=		1800
16	6′-dehydroxy-*S*-deoxo-Ala[6]-amanullin	=	=	$-CH(CH_3)CH_2CH_3$	H	=	CH_3	=	=		5600
17	6′-dehydroxy-*S*-deoxo-Ala[7]-amanullin	=	=	$-CH(CH_3)CH_2CH_3$	H	=	=	CH_3	=		28

[a] "=" indicates that the specific functional group is identical with the corresponding group in α-amanitin. [b] sBu is *sec*-butyl ($-CH(CH_3)CH_2CH_3$). [c] It should be mentioned that recent toxicological studies with compounds **1**, **2**, **3**, **4**, 7, **9**, and **11** (and perhaps not an identical race of mice) showed slightly higher LD_{50} values of 0.4–0.8, 0.5–1.0, 0.4, 20, 20, 0.8, and >50, respectively; Wieland, Th., personal correspondance.

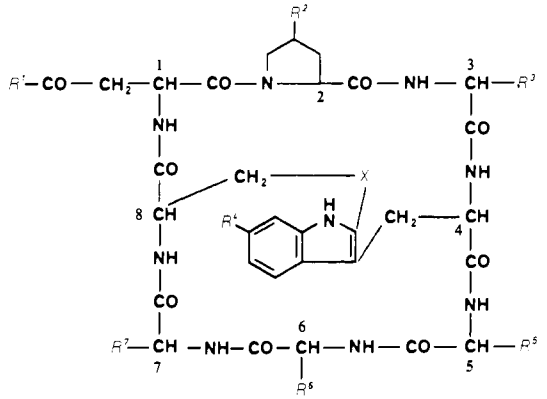

Figure 1. General chemical structure of the amatoxins (see Table I).

is presented in Figure 1, and the specific compositions of six of the nine naturally occurring ones (compounds **1**–**6**) are listed in Table I. The natural amatoxins are composed of the same amino acid bicyclic frame but differ in the numer of hydroxyl groups and the nature of side chain 1 (Asp/Asn). With the exception of Proamanullin, the other eight compounds are four acid-amide pairs.

In addition to the naturally occurring amatoxins, more than 40 amatoxin derivatives have been prepared by chemical modification of the natural amatoxins and by total syntheses;[3,6,7,13] several of these derivatives are listed in Table I (compounds **7**–**17**). The combined family of natural and synthetic amatoxins exhibits interesting structure–activity relationships.

Although the bicyclic backbone and most of the principal features are preserved across these series of compounds, the in vitro activity (K_i) and the in vivo effect (LD_{50}) vary significantly. As can be seen from the sample data (17 amatoxins) given in Table I, K_i's range between 0.23×10^{-8} and 5×10^{-5} M, whereas LD_{50}'s can measure below 0.5 mg/kg (very toxic) and above 100 mg/kg (nontoxic). Structural differences as small as a single hydroxyl group (e.g. **4** vs **5**) or a single methyl group (e.g. **12** vs **13**) in certain positions result in a 10–1000-fold change in the binding affinity to RNA polymerase B (K_i), and also yield similar changes in toxicity.

From the correlation between the chemical composition and the biological activity of the amatoxins, several conclusions were drawn: (1) The bicyclic frame is required for strong inhibition.[6,7] (2) The hydroxyl group of the hydroxy proline (side chain 2) is essential for activity.[6,7] (3) The chemical nature of side chain 3 is crucial for binding and toxicity. For maximum inhibition the β-methyl and the γ-hydroxyl are necessary.[6,7,13] (4) Side chains 5 (Gly) and 6 (Ile) might be located in the contact region with the enzyme.[13] (5) The chemical nature of the sulfur bridge affects the activity, especially the absolute configuration of the sulfoxide group[13,14] ((*R*) being more active than (*S*)).

In addition, from CD and ORD analyses of several amatoxin derivatives[15] in solution, it was concluded that the overall conformation is very important for activity. Likewise, kinetic and thermodynamic data of amatoxin–enzyme complex formation suggest that hydrogen bonds as well as hydrophobic forces are involved in the interactions between amatoxins and RNA polymerase B.[10]

However, it is not as yet clear to what extent the change in chemical structure of certain side chains directly affects the binding affinity of amatoxins to the enzyme. Indirect effects due to conformational changes in the amatoxin molecule could be responsible; the net effect could also be a combination of these effects.

In order to determine the importance of the specific functional groups for the overall conformation of amatoxins, and in an attempt to understand the relationships among chemical composition, three-dimensional structure, and biological function of amatoxins, a series of X-ray structural analyses of amatoxin derivatives was undertaken.

So far the detailed crystallographic analyses of four different amatoxin derivatives have been completed: β-amanitin (**2**), the (*S*)-sulfoxide isomer of 6′-*O*-methyl-α-amanitin (**7**), sulfone of 6′-*O*-methyl-α-amanitin (**8**), and *S*-deoxo-Ile[3]-amaninamide (**10**). The complete crystal structures of **2**[16] and **10**[17] have been reported, and the preliminary structures of **7** and **8** have been presented elsewhere.[14] Here we present the details of the final crystal structures of **7** and **8**, including solvent molecules, and we compare the overall conformation, intramolecular hydrogen bonds, and intermolecular interactions in the four amatoxin crystal structures with regard to their activity.

Experimental Section

A preliminary report[14] presented some of the experimental details of the crystallization, data collection, and earlier stages of the structure determination of 7 and **8**. A summary of the final crystallographic data

(13) Wieland, Th.; Götzendörfer, C.; Zanotti, G.; Vaisius, A. C. *Eur. J. Biochem.* **1981**, *117*, 161.

(14) Wieland, Th.; Götzendörfer, C.; Dabrowski, J.; Lipscomb, W. N.; Shoham, G. *Biochemistry* **1983**, *22*, 1264.

(15) Faulstich, H.; Bloching, M.; Zobeley, S.; Wieland, Th. *Experimentia* **1973**, *29*, 1230.

(16) Kostansek, E. C.; Lipscomb, W. N.; Yocum, R. R.; Thiessen, W. E. *Biochemistry* **1978**, *17*, 3790.

(17) Shoham, G.; Rees, D. C.; Lipscomb, W. N.; Zanotti, G.; Wieland, Th. *J. Am. Chem. Soc.* **1984**, *106*, 4606.

Table II. Crystallographic Data for the Structural Studies of 7, **8**, **10**, and **2**

parameter	7	**8**	**10**	**2**
crystallized from	methanol	90% ethanol	90% ethanol	95% ethanol
space group	$P2_12_12_1$	$P2_12_12_1$	$P2_1$	$P2_12_12_1$
a, Å	15.883 (2)	16.123 (3)	12.147 (1)	14.004 (3)
b, Å	18.245 (2)	18.358 (4)	11.250 (1)	14.943 (3)
c, Å	20.247 (3)	20.119 (5)	19.267 (1)	30.794 (7)
β, deg	90.0	90.0	92.41 (1)	90.0
v, Å^3	5867 (1)	5955 (2)	2630.5 (3)	6444 (4)
Z	4	4	2	4
MW (peptide)	933.02	949.01	854.99	919.97
solvent in asym unit	$1H_2O$ 6MeOH	$4H_2O$ 3EtOH	$3H_2O$ 2EtOH	$7H_2O$ 3EtOH
ρ_{calc}	1.26	1.23	1.26	1.11
observations	5007	4839	3894	3395
refined param	856	795	814	749
R	0.063	0.068	0.065	0.10

for 7 and **8** along with the corresponding data for **2** and **10** is presented in Table II. For all four derivatives the crystallographic data were collected from one single crystal sealed in a glass capillary with a small amount of mother liquor. The intensity data for 7, **8**, and **2** were measured on a Syntex-$P2_1$ diffractometer with graphite monocromated Cu Kα radiation (λ = 1.541 78 Å), whereas the data for **10** were measured on a Nicolet-R3m diffractometer with graphite monochromated Mo Kα radiation (λ = 0.710 69Å). Unfortunately, in all four cases the crystals were too delicate to determine an experimental density. This parameter could be of particular interest in the case of **2** since its calculated density deviates somewhat from the mean value of the other derivative and its final crystallographic R factor is somewhat larger than the values obtained for the other derivatives.

Refinement. In the preliminary structures of 7 and **8** described earlier,[14] the refined model included only non-hydrogen atoms and only the part of the data for which $F_o \geq 4.0\sigma(F_o)$. The preliminary refinement resulted in crsytallographic R factors of 0.075 and 0.076 for 7 and **8**, respectively.

For the final structures of 7 and **8** presented here, all of the peptide hydrogen atoms and most of the solvent molecules hydrogen atoms were introduced onto the preliminary models. A more restricted refinement of the geometries of the solvent molecules and their statistical occupancies together with the larger data sets used resulted in better agreement factors (R) and better structural parameters for both 7 and **8**.

Structural Refinement of 7. For the refinement of the structure of 7 ($C_{40}H_{56}N_{10}O_{14}S\cdot H_2O\cdot 5.15$MeOH), those 5007 reflections with $F_o \geq 2.0\sigma(F_o)$, 92% of all the independent data collected, were used. A few rounds of blocked least-squares refinement[18] and F_o–F_c Fourier maps, using the preliminary model[14] as the starting point, enabled the completion of the model with hydrogen atoms. Of the 56 hydrogen atoms of the peptide, 44 were observed with reasonable electron density in the difference maps. The other 12 H atoms, belonging to the 4 methyl groups in the molecule, had to be constructed geometrically. In the final stage of refinement, positions of most peptide hydrogens were refined independently, except for the hydrogens of the NH_2 group of side chain 1, the methyl groups of side chains 4 and 6, and all hydrogens of side chain 3, all of which had to be constrained at a fixed distance from the corresponding non-hydrogen atoms.

Seven solvent molecules ($1H_2O$ and 6MeOH) have been found in the crystallographic asymmetric unit. The water molecule (W1) and four methanol molecules (M1–M4) were assigned full occupancy. The fifth methanol molecule (M5) was assigned partial occupancy of 0.7, whereas the sixth methanol molecule (M6) was found to be disordered between two positions (M6 and M61) with partial occupancies of 0.3 and 0.15, respectively. Of the solvent hydrogen atoms, those of the water molecule and the hydroxyl groups of M1–M5 have been located from the difference maps. The hydrogens of the methyl groups of methanol were constructed geometrically. No hydrogen atoms were assigned to M6 because of the low occupancy. All solvent and peptide hydrogens were refined with isotropic temperature factors; however, the positional parameters of all constructed hydrogens were not refined independently. All non-hydrogen atoms were assigned anisotropic temperature factors, except the atoms of M6 and M61, which were refined with isotropic temperature factors.

The refinement converged smoothly to a final R factor of 0.063. In the final cycle of refinement, the largest ratio of shift to estimated standard deviation (esd) in the atomic parameters was less than 0.09 (av of 0.006), and the final difference synthesis displayed no peaks greater than 0.34 e/Å^3 (min., −0.26 e/Å^3) in the solvent region or 0.25 e/Å^3 around the peptide. In the final structure, bond lengths between non-hydrogen and hydrogen atoms are in the range of 0.7–1.2 Å with a mean of 0.96 Å.

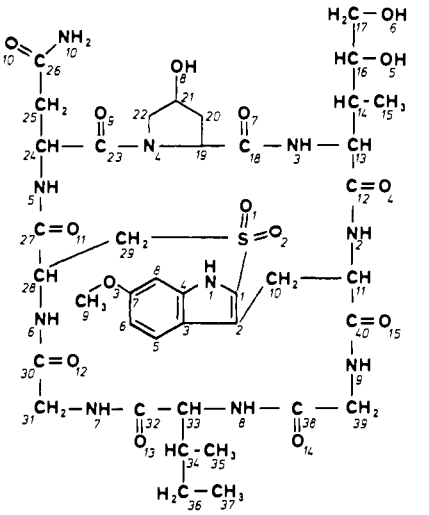

Figure 2. Chemical structure and numbering scheme for derivative **8**. The same numbering scheme is used here for derivatives 7, **10**, and **2**, respectively, except that N_{10} is replaced by O_{16} in **2**.

Structural Refinement of 8. For the refinement of the structure of **8** ($C_{40}H_{56}N_{10}O_{15}S\cdot 2.5H_2O\cdot 2.35$EtOH), those 4846 reflections with $F_o \geq 2.0\sigma(F_o)$, 88% of all the independent data collected, were used. After a few cycles of difference electron density maps and block-diagonal least-squares refinement[18] all the peptide hydrogen atoms, except those of the four methyl groups and some of the solvent hydrogen atoms, were revealed. The peptide methyl groups and the rest of the solvent hydrogens were then constructed geometrically and a few cycles of full-matrix least-squares refinement were allowed.

The positions of the hydrogen atoms of the tryptophan 6′-methoxy group, the hydrogens of the asparagine terminal NH_2 group, and all the hydrogen atoms in side chains 3 and 6 displayed some degree of instability during the refinement; thus only their thermal parameter, but not their positions, were refined independently in the final stage of the refinement.

Of the accompanying four water and three ethanol molecules, only one water molecule (W1) and one ethanol molecule (E1) were refined in full occupancy. The other solvent molecules were refined to fractional occupancies of 0.5, 0.6, and 0.4 for W2, W3, and W4, respectively, and of 0.75 and 0.6 for E2 and E3, repectively. Because of instability during the refinement and large thermal parameters, all seven solvent molecules were refined as rigid bodies in the final stages, and in the ethanol molecules only the hydroxyl hydrogens were considered for the final model. All the non-hydrogen atoms in the crystal structure were refined with anisotropic thermal parameters.

The refinement converged to a final R factor of 0.068. In the final cycle of refinement, the largest ratio of shift/esd was 0.2 (av of 0.03) and the highest peaks in the difference electron density map were 0.39 e/Å^3 (min., −0.22 e/Å^3) in the solvent region, and 0.20 e/Å^3 around the peptide. In the final structure, bond lengths between non-hydrogen and hydrogen atoms are in the range of 0.7–1.2 Å with a mean of 0.99 Å.

In both crystal structures (7 and **8**) the relatively low noise level in the difference maps and the almost constant agreement factor (R) as a function of resolution indicate that we accounted for all of the solvent molecules present in the crystal structure, at least those with significant occupancies.

Results

The final fractional coordinates for all non-hydrogen atoms in the crystal structures of 7 and **8** are listed in Tables III and IV, respectively.[19] The numbering scheme for both molecules is identical (except, of course, for the addition of O2 in the sulfone **8**) and is presented in Figure 2. The same numbering system is also used later for **2** and **10**, for comparison, whereas N10 of

(18) Sheldrick, G. *Programs for Crystal Structure Determination*; Cambridge: England, 1975.

(19) For anisotropic thermal parameters for non-hydrogen atoms and positional and thermal parameters for hydrogen atoms, see supplementary material.

Table III. Positional Parameters for Non-H Atoms in the Crystal Structure of 7

	x/a	y/b	z/c		x/a	y/b	z/c
C1	0.0036 (3)	0.8789 (3)	0.8278 (2)	N1	0.0069 (3)	0.9232 (2)	0.8834 (2)
C2	−0.0766 (3)	0.8531 (3)	0.8179 (2)	N2	−0.2002 (3)	0.7707 (2)	0.6761 (2)
C3	−0.1267 (3)	0.8836 (3)	0.8713 (2)	C3	−0.2075 (3)	0.6956 (2)	0.5574 (2)
C4	−0.0721 (3)	0.9270 (3)	0.9094 (2)	N4	−0.0464 (2)	0.7223 (2)	0.5030 (2)
C5	−0.2113 (4)	0.8771 (3)	0.8906 (2)	N5	0.1057 (3)	0.7696 (2)	0.6315 (2)
C6	−0.2380 (4)	0.9152 (4)	0.9455 (3)	N6	0.1714 (3)	0.9619 (2)	0.6288 (2)
C7	−0.1820 (4)	0.9590 (3)	0.9822 (3)	N7	0.1656 (3)	1.0908 (2)	0.5644 (2)
C8	−0.0990 (4)	0.9657 (3)	0.9657 (2)	N8	−0.0528 (3)	1.0946 (2)	0.5926 (2)
C9	−0.1699 (5)	1.0468 (4)	1.0687 (4)	N9	−0.1365 (3)	0.9233 (2)	0.6605 (2)
C10	−0.1051 (4)	0.8000 (3)	0.7661 (2)	N10	0.0238 (3)	0.6249 (3)	0.7280 (2)
C11	−0.1870 (3)	0.8220 (3)	0.7309 (2)	O1	0.1063 (3)	0.7806 (2)	0.7736 (2)
C12	−0.2767 (3)	0.7558 (3)	0.6523 (2)	O3	−0.2178 (3)	0.9927 (3)	1.0363 (2)
C13	−0.2797 (3)	0.6916 (3)	0.6026 (2)	O4	−0.3407 (2)	0.7866 (2)	0.6704 (2)
C14	−0.2823 (4)	0.6155 (3)	0.6375 (2)	O5	−0.2773 (3)	0.5524 (2)	0.5292 (2)
C15	−0.3334 (6)	0.6181 (4)	0.7017 (3)	O6	−0.3644 (4)	0.4304 (2)	0.5792 (2)
C16	−0.3208 (4)	0.5576 (3)	0.5904 (2)	O7	−0.2572 (2)	0.7973 (2)	0.5070 (2)
C17	−0.3188 (5)	0.4803 (3)	0.6195 (3)	O8	−0.0062 (3)	0.7513 (2)	0.3599 (2)
C18	−0.2011 (3)	0.7515 (3)	0.5145 (2)	O9	−0.0513 (2)	0.8011 (2)	0.5875 (2)
C19	−0.1231 (3)	0.7533 (3)	0.4721 (2)	O10	−0.0803 (2)	0.6495 (2)	0.6579 (2)
C20	−0.1320 (4)	0.7075 (4)	0.4100 (3)	O11	0.1407 (2)	0.8474 (2)	0.5503 (1)
C21	−0.0420 (4)	0.6893 (4)	0.3910 (3)	O12	0.3061 (3)	0.9776 (2)	0.6630 (2)
C22	−0.0002 (4)	0.6730 (3)	0.4568 (2)	O13	0.0999 (3)	1.1277 (2)	0.6571 (2)
C23	−0.0143 (3)	0.7512 (3)	0.5582 (2)	O14	0.0018 (2)	0.9795 (2)	0.5928 (2)
C24	0.0687 (3)	0.7196 (3)	0.5836 (2)	O15	−0.2307 (3)	0.9461 (2)	0.7400 (2)
C25	0.0588 (4)	0.6426 (3)	0.6141 (3)	S	0.1012 (1)	0.8600 (1)	0.7900 (1)
C26	−0.0052 (4)	0.6394 (3)	0.6687 (2)	OW1[a]	−0.1092 (4)	0.5088 (4)	0.5298 (3)
C27	0.1337 (3)	0.8346 (3)	0.6103 (2)	OM1	0.4524 (3)	1.0200 (4)	0.6044 (3)
C28	0.1567 (3)	0.8933 (3)	0.6625 (2)	CM1	0.4867 (8)	1.0821 (8)	0.6286 (7)
C29	0.0836 (4)	0.9054 (3)	0.7126 (3)	OM2	−0.1848 (4)	1.1814 (3)	0.6416 (3)
C30	0.2436 (4)	0.9984 (3)	0.6325 (3)	CM2	−0.2674 (7)	1.1894 (8)	0.6226 (6)
C31	0.2424 (4)	1.0728 (3)	0.5976 (3)	OM3	−0.2072 (4)	1.0905 (4)	0.7836 (3)
C32	0.0981 (4)	1.1156 (3)	0.5973 (3)	CM3	−0.2721 (8)	1.1126 (8)	0.8167 (8)
C33	0.0184 (4)	1.1257 (3)	0.5567 (3)	OM4	−0.5353 (5)	0.4743 (4)	0.5859 (3)
C34	0.0011 (5)	1.2081 (3)	0.5433 (3)	CM4	−0.5609 (8)	0.5470 (6)	0.5624 (5)
C35	0.0786 (5)	1.2443 (4)	0.5128 (4)	OM5[b]	−0.3878 (5)	0.9365 (6)	0.8010 (4)
C36	−0.0762 (6)	1.2174 (4)	0.4991 (5)	CM5	−0.4356 (9)	0.9365 (13)	0.7565 (8)
C37	−0.1117 (8)	1.2926 (5)	0.4993 (6)	OM6[c]	−0.4148 (20)	0.3257 (16)	0.6777 (15)
C38	−0.0556 (4)	1.0220 (3)	0.6067 (3)	CM6	−0.3546 (21)	0.3183 (18)	0.7254 (16)
C39	−0.1335 (4)	0.9998 (3)	0.6417 (3)	OM61	−0.4261 (25)	0.2461 (21)	0.7297 (19)
C40	−0.1867 (3)	0.9028 (3)	0.7100 (2)	CM61	−0.5038 (40)	0.2743 (33)	0.6856 (29)

[a] $W_1 \rightarrow$ M6 are the 7 solvent molecules (W = water, M = methanol). [b] The occupancy of M5 is 0.7. [c] M6 and M61 are two disordered positions of M6 with partial occupancies of 0.3 and 0.15, respectively.

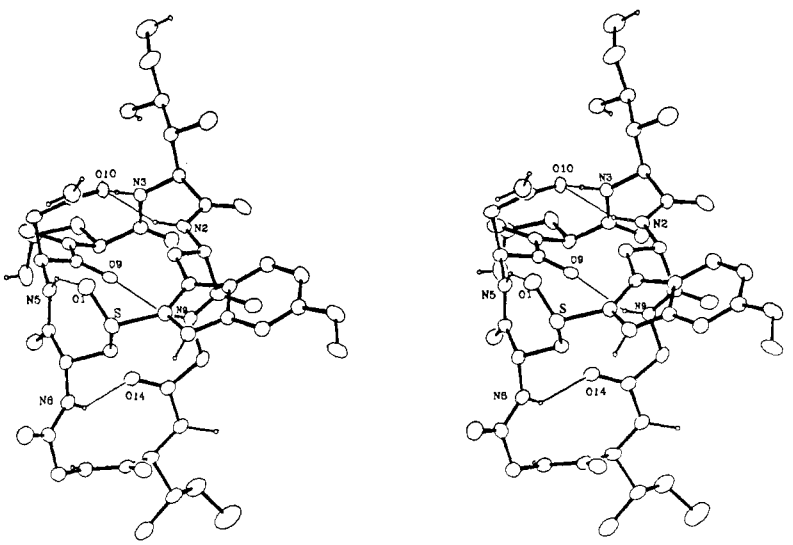

Figure 3. Stereo drawing of the molecular structure and intramolecular hydrogen bonds (thin lines) in 7.

the Asn-1 side chain is replaced by O16 (Asp-1) in **2**. Stereo drawings[20] of molecules **7** and **8**, and their intramolecular hydrogen bonds, are given in Figures 3 and 4, respectively. The molecular orientation in these two figures is intentionally different, in order to show these two structures (which are similar) from two different viewpoints.

Molecular Structure of 7 and 8. The molecular structures of **7** and **8** are almost identical, and their overall conformation is similar, for the most part, to that in **2** and **10**. As in the crystal structure of **2** and **10**, and probably as in most of the amatoxins, the primary 24-membered macrocycle in **7** and **8** is "bent" at the bridging points. The bridging indole–sulfoxide/sulfone segment

(20) Johnson, C. K. *ORTEP-II, a Fortran Thermal-Ellipsoid Plot Program for Crystal Structure Illustrations*; Oak Ridge National Laboratory Report ORNL-5138, 1976.

Table IV. Positional Parameters for Non-H Atoms in the Crystal Structure of **8**

	x/a	*y/b*	*z/c*		*x/a*	*y/b*	*z/c*
C1	0.0002 (3)	0.8794 (3)	0.8287 (3)	C40	−0.1840 (4)	0.8988 (3)	0.7112 (3)
C2	−0.0780 (3)	0.8511 (3)	0.8225 (2)	N1	0.0055 (3)	0.9269 (2)	0.8834 (2)
C3	−0.1245 (3)	0.8815 (3)	0.8769 (3)	N2	−0.1972 (3)	0.7680 (2)	0.6785 (2)
C4	−0.0702 (3)	0.9276 (3)	0.9128 (3)	N3	−0.2023 (3)	0.6952 (2)	0.5582 (2)
C5	−0.2058 (4)	0.8721 (4)	0.9012 (3)	N4	−0.0422 (3)	0.7187 (2)	0.5035 (2)
C6	−0.2282 (5)	0.9051 (4)	0.9588 (4)	N5	0.1085 (3)	0.7671 (2)	0.6319 (2)
C7	−0.1721 (4)	0.9524 (4)	0.9928 (3)	N6	0.1658 (3)	0.9591 (2)	0.6241 (2)
C8	−0.0941 (4)	0.9633 (3)	0.9710 (3)	N7	0.1572 (4)	1.0879 (3)	0.5609 (3)
C9	−0.1630 (5)	1.0429 (5)	1.0764 (4)	N8	−0.0559 (3)	1.0883 (2)	0.5924 (2)
C10	−0.1054 (4)	0.7973 (3)	0.7716 (3)	N9	−0.1367 (3)	0.9166 (2)	0.6585 (2)
C11	−0.1858 (3)	0.8194 (3)	0.7337 (2)	N10	0.0235 (4)	0.6216 (3)	0.7297 (3)
C12	−0.2713 (3)	0.7544 (3)	0.6529 (3)	O1	0.0951 (3)	0.7828 (2)	0.7737 (2)
C13	−0.2747 (3)	0.6915 (3)	0.6026 (2)	O2	0.1576 (2)	0.8938 (3)	0.8216 (2)
C14	−0.2791 (4)	0.6156 (3)	0.6373 (2)	O3	−0.2055 (3)	0.9823 (3)	1.0485 (3)
C15	−0.3267 (6)	0.6204 (4)	0.7029 (3)	O4	−0.3350 (2)	0.7870 (2)	0.6691 (2)
C16	−0.3200 (4)	0.5594 (3)	0.5907 (3)	O5	−0.2783 (3)	0.5533 (2)	0.5292 (2)
C17	−0.3219 (6)	0.4828 (4)	0.6188 (4)	O6	−0.3714 (3)	0.4361 (2)	0.5778 (2)
C18	−0.1938 (4)	0.7508 (3)	0.5156 (3)	O7	−0.2477 (2)	0.7970 (2)	0.5074 (2)
C19	−0.1168 (3)	0.7516 (3)	0.4737 (3)	O8	0.0017 (3)	0.7510 (3)	0.3630 (2)
C20	−0.1267 (4)	0.7087 (4)	0.4080 (3)	O9	−0.0455 (2)	0.7961 (2)	0.5899 (2)
C21	−0.0379 (4)	0.6881 (4)	0.3898 (3)	O10	−0.0756 (2)	0.6491 (2)	0.6580 (2)
C22	−0.0010 (5)	0.6688 (4)	0.4564 (3)	O11	0.1426 (3)	0.8431 (2)	0.5494 (2)
C23	−0.0108 (3)	0.7476 (3)	0.5597 (3)	O12	0.3000 (3)	0.9762 (3)	0.6582 (2)
C24	0.0726 (3)	0.7154 (3)	0.5849 (3)	O13	0.0954 (3)	1.1241 (2)	0.6554 (2)
C25	0.0623 (4)	0.6387 (3)	0.6168 (4)	O14	−0.0020 (3)	0.9749 (2)	0.5867 (2)
C26	−0.0037 (4)	0.6363 (3)	0.6696 (3)	O15	−0.2242 (3)	0.9434 (2)	0.7429 (2)
C27	0.1343 (3)	0.8311 (3)	0.6081 (3)	S	0.0913 (1)	0.8605 (1)	0.7860 (1)
C28	0.1525 (3)	0.8904 (3)	0.6604 (3)	OW1[b]	−0.1090 (3)	0.5111 (3)	0.5319 (3)
C29	0.0778 (4)	0.9034 (3)	0.7084 (3)	OW2	−0.2148 (8)	1.0936 (6)	0.7749 (6)
C30	0.2372 (4)	0.9966 (3)	0.6286 (3)	OW3	−0.2084 (11)	0.9034 (9)	0.4044 (7)
C31	0.2350 (4)	1.0710 (3)	0.5923 (4)	OW4	−0.0770 (19)	0.9583 (16)	0.4264 (14)
C32	0.0913 (4)	1.1120 (3)	0.5955 (3)	OE1	0.4463 (3)	1.0174 (3)	0.6034 (3)
C33	0.0136 (4)	1.1214 (3)	0.5570 (3)	C1E1	0.4801 (3)	1.0817 (3)	0.6378 (3)
C34	−0.0052 (5)	1.2053 (3)	0.5460 (4)	C2E1	0.5170 (3)	1.0611 (3)	0.7005 (3)
C35	0.0699 (6)	1.2392 (5)	0.5122 (4)	OE2	−0.1855 (5)	1.1694 (3)	0.6607 (4)
C36	−0.0868 (6)	1.2148 (4)	0.5042 (5)	C1E2	−0.2745 (5)	1.1719 (3)	0.6491 (4)
C37	−0.1181 (7)	1.2939 (5)	0.5047 (7)	C2E2	−0.3064 (5)	1.2450 (3)	0.6761 (4)
C38	−0.0587 (4)	1.0170 (3)	0.6035 (3)	OE3	−0.4810 (13)	0.3624 (9)	0.6810 (8)
C39[a]	−0.1368 (5)	0.9933 (5)	0.6403 (8)	C1E3	−0.5533 (13)	0.3290 (9)	0.7030 (8)
C039	−0.1389 (5)	0.9819 (5)	0.6161 (8)	C2E3	−0.6064 (13)	0.3901 (9)	0.7111 (8)

[a] C39 and C039 are the 2 disordered positions of C39 with partial occupancies of 0.7 and 0.3, respectively. [b] W1 → E3 are the 7 solvent molecules (W = water, E = ethanol). Occupancies are 1.0, 0.5, 0.6, 0.4, 1.0, 0.75, and 0.6 for W1, W2, W3, W4, E1, E2, and E3, respectively.

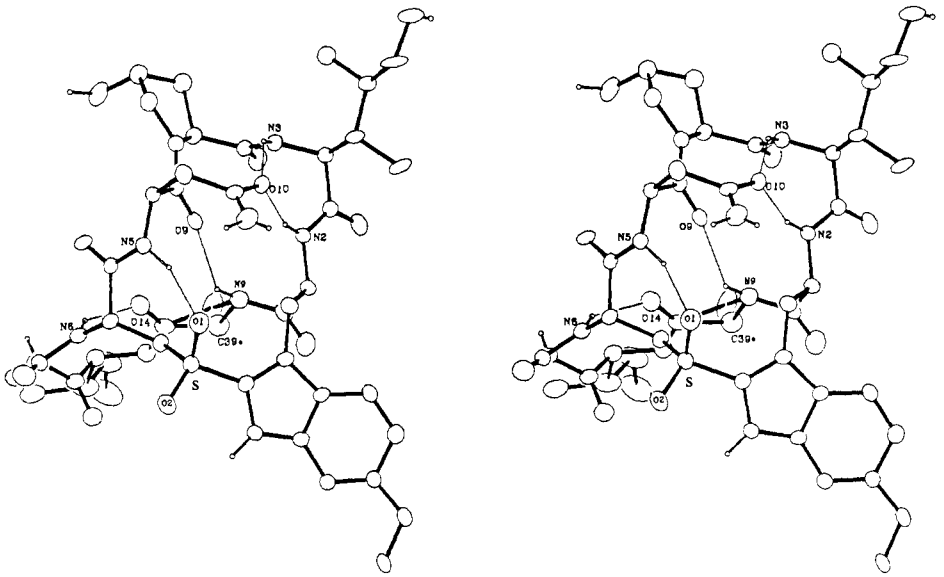

Figure 4. Stereo drawing of the molecular structure and intramolecular hydrogen bonds (thin lines) in **8**; C39* indicates the two disordered positions of C39.

divides the large macrocycle into two 18-membered rings, designated ring 1 and ring 2. Ring 1 is composed of Asn-1, HyPro-2 (γ-hydroxyproline), DihyIle-3 ((γ,δ)-dihydroxyisoleucine), and the common sulfur (sulfoxide/sulfone) bridge, possessing a relatively hydrophilic nature; ring 2 contains, in addition to the sulfur bridge, the amino acids Gly-5, Ile-6, and Gly-7, resulting in a more hydrophobic nature. Both rings are relatively "flat" and the dihedral angle between their least-squares planes (lsp's) is about 75°. The overall shape of the molecules can be described as distorted "T" or "flat Y". The indole ring lies roughly in the same plane as ring 1 (the dihedral angle between the two planes is about 30°) forming the top part of the "T" or "Y", and the 13-membered

Table V. Backbone Torsion Angles in 7, **8**, **10**, and **2**

parameter	residue no. 1	2	3	4	5	6	7	8
(1) φ_i								
7	−68	−61	−66	−81	157	−63	79	−122
8	−67	−62	−66	−81	155	−64	78	−121
10	−172	−68	−99	−76	118	−48	83	−134
2	−172	−60	−79	−109	140	−59	87	−121
(2) ψ_i								
7	164	−31	−41	−52	−177	134	−2	−171
8	162	−31	−42	−46	−174	133	1	−170
10	179	−17	−48	−27	−168	131	1	−76
2	179	−37	−23	−40	−178	127	−3	−85
(3) ω_i								
7	−175	177	−171	−178	−178	−175	−175	168
8	−174	178	−171	−179	−179	−175	−174	166
10	−174	−179	180	166	−180	179	−166	178
2	−174	−172	−169	172	−175	−176	−173	179

segment of the peptide backbone of ring 2 (residues 4→8), which is approximately perpendicular to the plane of the top part, forms the stem of the "T" (or "Y"). The amino acid side chains are located at the corners of the macrocycles, pointing generally away from the center of the peptide ring, as has been observed in similar cyclic peptides.[21]

The backbone bond lengths and bond angles in **7** and **8**, together with the corresponding parameters in **10**[17] and **2**,[16] are listed in Tables S7 and S8 (supplementary material), respectively. Several sets of "standard" peptide unit dimensions, based on accurate crystal structures of small peptides[22-25] and average parameters in protein crystal structures,[26,27] have been reported in the last 3 decades. These "normal" peptide unit bond lengths range between 1.449–1.470, 1.510–1.530, 1.229–1.260, and 1.310–1.335 Å for N_i–C_i^α, C_i^α–C_i, C_i–O_i, and C_i–N_{i+1}, respectively (nomenclature used is that defined in ref 28). The "normal" peptide unit bond angles range between 121.9–123.1°, 110.0–113.0°, 114.0–116.6°, 120.0–121.1°, and 122.9–125.0° for C_{i-1}–N_i–C_i^α, N_i–C_i^α–C_i, C_i^α–C_i–N_{i+1}, C_i^α–C_i–O_i, and O_i–C_i–N_{i+1}, respectively.

A comparison has been made between the average values for the structural parameters of the peptide unit in the amatoxin derivatives and the corresponding "normal" values reported in ref 25, which are the weighted average parameters calculated from 34 small peptide structures (Tables S7 and S8). A few individual bond lengths and bond angles in the peptide backbone of **7** and **8** (as well as in **10** and **2**) deviate somewhat from the average or from the corresponding acceptable ranges; however, the averages of these values (with their experimental sd's) are within the ranges mentioned above and are very similar to the values listed in ref 25. This indicates that no crystallographic artifacts ("bad" data, abnormal solvent interaction, or abnormal crystal forces, etc.), and more importantly, no unusual intracyclic strains, are affecting the crystal structures of **7** and **8** to a significant degree.

Backbone torsion angles (as defined in ref 28) of **7** and **8** are listed along with those of **10** and **2** in Table V. The ϕ,ψ values of all six non-Gly residues in **7** and **8** lie within the allowed ("outer limit"[29]) regions of a Ramachandran plot.[29,30] The conformation parameters (ϕ,ψ) of residues 2, 3, and 4 fall into the "α-helix" region in the above diagram,[29] resulting in a small "α-helical-like" stretch, whereas the conformational parameters of residues 1, 6, and 8 fall generally into the "β-sheet" region in this diagram (8 being on the edge of the unallowed region). The conformations of the more flexible glycines residues (5 and 7) are similar to those usually observed in proteins[30,31] and peptides.[32] An indication of the flexibility of the glycine residues is the disorder seen in the C^α of Gly 5 (C39) in the crystal structure of **8**. The two partially occupied positions (C39 and C039) are 0.53 Å apart related by a rotation on an axis parallel to the peptide backbone. In Table V, as well as in Tables S7 and S8, only the structural parameters related to the more populated position (C39, 0.7) are presented; the torsion angles ω_4, ϕ_5, ψ_5, and ω_5 (Table V) differ by 10–20° for the less populated position (C039, 0.3).

Table VI. Side Chain Torsion Angles in 7, **8**, **10**, and **2**

parameter	torsion angle	7	**8**	**10**	**2**
Asn/Asp 1					
χ^1	N5–C24–C25–C26	68	69	64	61
$\chi^{2,1}$	C24–C25–C26–O10	66	62	45	26
HyPro 2					
χ^1	N4–C19–C20–C21	−32	−30	−30	−31
$\chi^{2,1}$	C19–C20–C21–O8	−78	−77	−76	−76
$\chi^{2,2}$	C19–C20–C21–C22	41	40	42	38
$\chi^{3,2,1}$	O8–C21–C22–N4	85	81	78	85
$\chi^{3,2,2}$	C20–C21–C22–N4	−32	−34	−38	−30
χ^4	C21–C22–N4–C19	12	16	20	12
DihyIle/Ile 3					
$\chi^{1,1}$	N3–C13–C14–C16	−80	−82	−73	−145
$\chi^{1,2}$	N3–C13–C14–C15	159	155	157	83
$\chi^{2,1}$	C13–C14–C16–O5	56	57		56
$\chi^{2,2}$	C13–C14–C16–C17	175	176	−49[a]	−179
χ^3	C14–C16–C17–O6	172	171		−177[b]
MeOTrp/HyTrp/ Trp 4					
χ^1	N2–C11–C10–C2	172	171	175	168
$\chi^{2,1}$	C11–C10–C2–C1	−135	−130	−131	−128
$\chi^{3,1}$	C10–C2–C1–N1	−176	−178	−173	−174
Ile 6					
$\chi^{1,1}$	N8–C33–C34–C36	−63	−60	−74	−66
$\chi^{1,2}$	N8–C33–C34–C35	174	177	162	170
χ^2	C33–C34–C36–C37	163	168	169	161

[a] In **10**, C17 is disordered; the torsion angle given is for the highest occupied (0.5) C17 position. [b] In **2**, O6 is disordered between 3 positions; the corresponding torsion angles are 60, −177, and −53.

All peptide bonds in **7** and **8** assume generally the common planar trans conformation.[22] The average torsion angle ω[28] in both structures is −179.1°, only 0.9° from the ideal trans conformation (ω = 180.0°). Individual ω angles deviate by −14° to +9° from 180°; however, six out of eight angles are within the 180 ± 5° range in **7** and within the 180 ± 6° range in **8**. It has been shown recently that nonplanar deformations of the amide unit with $|\Delta\omega|$ up to 15° are not uncommon,[25,33] and that these are rather probable, since the increase in energy for such deviations from planarity is only of the order of 0.5 kcal/mol.[33,34]

The rather usual conformational parameters and the lack of any significant distortion in the peptide backbone of **7** and **8** further indicate that these two rather compact bicyclic peptides are not experiencing noticeable strain or unusual intramolecular forces.

Side chain bond lengths and bond angles in the crystal structures of **7** and **8** are given in Tables S9 and S10 (supplementary material), respectively. The bond lengths and angles have been compared with the corresponding usual (and more accurate) parameters averaged from the crystal structure of the specific isolated amino acid[35-37] or small molecules.[38] Side chain bond

(21) Ovchinnikov, Y. A.; Ivanov, V. T. In *The Proteins*; Neurath, H., Hill, R. L., Eds.; Academic Press: New York, 1982; Vol. V, pp 307–642.
(22) Corey, R. B.; Pauling, L. *Proc. Roy. Soc.* **1953**, *B141*, 10.
(23) Marsh, R. E.; Donohue, J. *Adv. Protein Chem.* **1967**, *22*, 235.
(24) Ramachandran, G. N.; Kolaskar, A. S.; Ramakrishnan, C.; Sasisekharan, V. *Biochim. Biophys. Acta* **1974**, *359*, 298.
(25) Benedetti, E. In *Peptides*; Goodman, M., Meienhofer, J., Eds.; Wiley: New York, 1977; pp 257–273.
(26) Levitt, M. *J. Mol. Biol.* **1974**, *82*, 393.
(27) Marquart, M.; Walter, J.; Deisenhofer, J.; Bode, W.; Huber, R. *Acta Crystallogr.* **1983**, *B39*, 480.
(28) IUPAC-IUB Commission on Biochemical Nomenclature. *Biochemistry* **1970**, *9*, 3471.
(29) Ramachandran, G. N.; Ramakrishnan, C.; Sasisekharan, V. *J. Mol. Biol.* **1963**, *7*, 95. (Note the different ϕ, ψ definitions used in this reference.)
(30) Mandel, N.; Mandel, G.; Trus, B. L.; Rosenberg, J.; Carlson, G.; Dickerson, R. E. *J. Biol. Chem.* **1977**, *252*, 4619.
(31) Richardson, J. S. *Adv. Protein Chem.* **1981**, *34*, 167.
(32) Benedetti, E. In *Chemistry and Biochemistry of Amino Acids, Peptides, and Proteins*; Weinstein, B., Ed.; M. Dekker, Inc.: New York, 1982; Vol. 6, pp 105–184.
(33) Kolaskar, A. S.; Lakshminarayanan, A. V.; Sarathy, K. P.; Sasisekharan, V. *Biopolymers* **1975**, *14*, 1081.
(34) Winkler, F. K.; Dunitz, J. D. *J. Mol. Biol.* **1971**, *59*, 169.
(35) Gurskaya, G. V. *The Molecular Structure of Amino Acids*; Consultant Bureau: New York, 1968; and references therein.

Table VII. The Sulfur Bridge Geometry in **7**, **8**, **10**, and **2**, in Comparison with the Geometry of Similar Units in Two Model Compounds

parameter	7	8	10	2	Mod-1[a]	Mod-2[b]
(1) bond lengths (Å)						
C1–S	1.764	1.736	1.756	1.750	1.74	1.749
C_{29}–S	1.793	1.762	1.819	1.757	1.83	1.821[c]
S–O_1[d]	1.490	1.450				*e*
S–O_2		1.426		1.510		1.519
(2) bond angles (deg)						
C_1–S–C_{29}	98.7	104.2	99.7	96.9	103	96.0
C1–S–O_1	109.6	108.5				
C_1–S–O_2		107.5		107.0		108.9
C_{29}–S–O_1	105.2	107.1				
C_{29}–S–O_2		110.2		104.4		106.8
O_1–S–O_2		118.4				
(3) torsion angles (deg)						
C_{10}–C_2–C_1–S	−3.1	−4.3	2.9	0.8	−11	*f*
C_2–C_1–S–C_{29}	72.4	75.3	88.6	97.8	137	
C_1–S–C_{29}–C_{28}	−174.6	−177.8	−179.2	180.0	−107	
S–C_{29}–C_{28}–N_6	−139.6	−141.7	−171.3	−173.8	59	
S–C_{29}–C_{28}–C_{27}	101.6	101.2	61.8	61.9	63	
C_2–C_1–S–O_1	−37.3	−38.5				
C_2–C_1–S–O_2		−167.7		−154.8		

[a] Model compound **1**, an analogous small synthetic cyclic peptide with similar thioether unit; ref 46. [b] Model compound **2**, a synthetic sulfoxide derivative of L-tryptophan (acyclic); ref 47. [c] Usual paraffinic C–S bond length is 1.82 Å in thioethers and 1.80 Å in sulfones and sulfoxides; ref 38, p S-22. [d] O_1 is the (*S*)-oxygen and O_2 is the (*R*)-oxygen. [e] Usual S–O bond length is 1.49 Å in sulfoxides and 1.43 Å in sulfones; ref 38, p S-11. [f] No torsion angles are given (nor coordinates).

lengths in **7** and **8** are very similar and their values in both structures agree generally well with the usually observed values (Table S9). Small deviations are noticeable, however, in the bond lengths of side chains 4 and 6. In the Ile-6 side chain, the deviations of up to ±0.05 Å from usual could be accounted for by the relatively high thermal parameters of its carbon atoms in both **7** and **8** (Tables S3 and S4 of the supplementary material). In the indole ring of the MeOTrp-4 side chain the formal single bonds are generally longer and the formal double bonds are generally shorter than the corresponding ones in the structure of isolated tryptophan molecules[36,39] and in the structure of **10**.[17] This decrease in "aromaticity" of the indole ring in **7** and **8** is probably due to the sulfoxide/sulfone and the methoxy substituents on the indole ring in **7** and **8**, respectively, which somewhat localize the π-system in the indole ring. Nevertheless, the indole ring in both structures is very nearly planar as expected; the average atomic deviations from the indole lsp's in **7** and **8** are |0.01| and |0.02| Å, respectively. Side chain bond angles in **7** and **8** are very similar to the usually observed ones, (Table S10), which again indicates that the small deviations in bond lengths are not due to any significant molecular distortions.

Side chain torsion angles[28] in **7** and **8** are given with those in **10** and **2** in Table VI. In general the torsion angle values for the side chain tetrahedral carbons are close to the ideal, fully staggered, rotameric conformations of g^+, *t*, and g^- (χ = 60°, 180° and −60°, respectively),[40] whereas the torsion angles involving trigonal carbons, $\chi^{2,1}$ of residues 1 and 4, significantly deviate from the low-energy conformations where $\chi = \pm 90°$ or $\chi = \approx 0°$. More specifically, analysis of the distribution of specific side chain torsion angles in proteins[40,41] and peptides,[42] in agreement with computed favorable side chain conformations,[43] shows the following: (a) In side chains with no β-branching the g^- conformation ($\chi^1 \approx -60°$) occurs most frequently, followed by the *t* conformation ($\chi^1 \approx 180°$), whereas the g^+ conformation is the least favored. (b) In side chains with β-branching there is strong preference for a conformation in which one C^γ is in the g^- position and the other C^γ is in the *t* position (e.g. $\chi^{1,1} \approx -60°$, $\chi^{1,2} \approx 180°$). (c) The extended (*t*) conformation is highly favored for the rotation around the C^β–C^γ ($\chi^2 \approx 180°$). (d) In aromatic side chains a definite preference for $\chi^2 \approx \pm 90°$ is observed. (e) In Asn and Asp residues the side chain atoms (C^α–O^δ) tend to lie close to a plane which is perpendicular to the plane of the N,C^α,C atoms (where the usually observed χ^2 is ≈20°). The conformational deviations of side chains 1 (Asn) and 4 (Trp) in **7** and **8** from these more stable conformations are probably due to the side chain hydrogen bonding in Asn-1 and the bridging constraint in MeOTrp-4.

The proline ring of side chain 2 assumes the C_s–C^γ–exo[44] or "up"[36] conformation in which the atoms N, C^α, C^β, and C^δ are nearly co-planar (the mean deviations from the lsp are |0.05| and |0.04| Å in **7** and **8**, respectively) and the C^γ atom (C21) is displaced from this plane away from the carbonyl group (0.57 Å in **7**, 0.58 Å in **8**). The substituted hydroxyl group (O^δ) is axially positioned on C^γ, displaced away from the proline plane, in the same direction as C^γ, by 1.98 and 2.00 Å in **7** and **8**, respectively. Although this conformation may not be the most stable (as found by theoretical calculations[45]), this conformation of the proline ring is the more common[36,37] and is similar in **10**[17] and **2**.[16]

The geometries of the sulfur-containing bridge in **7** and **8** are compared in Table VII with those in **10** and **2** and in two model compounds.[46,47] In general it seems that none of the geometrical parameters of this unit in **7** and **8** are out of the ordinary; particularly the geometries of the sulfoxide (in **7**) and sulfone (in **8**) moieties agree rather well with the geometries of similar groups in small molecules[38] and the structures of dimethyl sulfoxide[48-50] and dimethyl sulfone,[51-53] respectively. We will compare the details of the geometry of this bridge in **7** and **8** with the other derivatives

(36) Momany, F. A.; McGuire, R. F.; Burgess, A. W.; Scheraga, H. A. *J. Phys. Chem.* **1975**, *79*, 2361; and references therein.
(37) Koetzle, T. F.; Lehmann, M. S.; Hamilton, W. C. *Acta Crystallogr.* **1973**, *B29*, 231.
(38) *Tables of Interatomic Distances and Configurations in Molecular and Ions*; Sutton, L. E., Sci. Ed.; The Chemical Society: London, 1965; Spec. Publ.-Chem. Soc. No. 18.
(39) Takigawa, T.; Ashida, T.; Sasada, Y.; Kakudo, M. *Bull. Chem. Soc. Jpn.* **1966**, *39*, 2369.
(40) Janin, J.; Wodak, S.; Levitt, M.; Meigret, B. *J. Mol. Biol.* **1978**, *125*, 357.
(41) Bhat, T. N.; Sasisekharan, V.; Vijayan, M. *Int. J. Peptide Protein Res.* **1979**, *13*, 170.
(42) Benedetti, E.; Morelli, G.; Némethy, G.; Scheraga, H. A. *Int. J. Peptide Protein Res.* **1983**, *22*, 1.
(43) Zimmerman, S. S.; Pottle, M. S.; Némethy, G.; Scheraga, H. A. *Macromolecules* **1977**, *10*, 1.
(44) Ashida, T.; Kakudo, M. *Bull. Chem. Soc. Jpn.* **1974**, *47*, 1129.
(45) Tanaka, S.; Scheraga, H. A. *Macromolecules* **1974**, *7*, 698.
(46) Wieland, Th.; Beijer, B.; Seeliger, A.; Dabrowski, J.; Zanotti, G.; Tonelli, A. E.; Gieren, A.; Dederer, B.; Lamm, V.; Hädicke, E. *Liebigs Ann. Chem.* **1981**, 2318.
(47) Wieland, Th.; Jordan de Urries, M. P.; Indest, H.; Faulstich, H.; Gieren, A.; Sturm, M.; Hoppe, W. *Liebigs Ann. Chem.* **1974**, 1570.
(48) Dreizler, H.; Dendl, G. *Z. Naturforsch.* **1964**, *19a*, 512.
(49) Viswamitra, M. A.; Kannan, K. K. *Nature* **1966**, *209*, 1016.
(50) Thomas, R.; Schomaker, C. B.; Eriks, K. *Acta Crystallogr.* **1966**, *21*, 12.
(51) Langs, D. A.; Silverton, J. V.; Bright, W. M. *J. Chem. Soc., Sect. D* **1970**, 1653.
(52) Saito, S.; Makino, F. *Bull. Chem. Soc. Jpn.* **1972**, *45*, 92.
(53) Hargittai, M.; Hargittai, I. *J. Mol. Struct.* **1974**, *20*, 283.

Table VIII. Intramolecular Hydrogen Bonds (<3.2 Å) in **7**, **8**, **10**, and **2**

no.	H bond from	to	or[a]	type	in	distances[b] N··O	distances[b] H··O	angles[c] N—H··O	angles[c] H··O=X	angles[c] N··O=X
(1)	N_5—H··O_9=C_{23}		1NH→10	2→2	7					
					8					
					10	2.61	2.16	107	87	66
					2	2.60	2.12	107	88	67
(2)	N_5—H··O_{14}=C_{38}		1NH→50	5→1	7					
					8					
					10	3.15	2.25	157	139	145
					2	3.16	2.44	128	138	152
(3)	N_5—H··O_1=S		1NH→80[δ1]	MC→SC[d]	7	2.83	2.33	141	114	107
					8	2.88	1.83	160	112	106
					10					
					2					
(4)	N_3—H··O_{10}=C_{28}		3NH→10[δ1]	MC→SC	7	2.99	2.40	126	134	145
					8	2.98	2.26	142	140	147
					10	2.93	2.21	148	141	149
					2					
(5)	N_2—H··O_{10}=C_{26}		4NH→10[δ1]	MC→SC	7	2.94	2.03	157	131	136
					8	2.96	2.02	162	133	139
					10	2.80	1.91	175	145	147
					2	3.15	2.40	130	157	169
(6)	N_9—H··O_9=C_{23}		5NH→10	5→1	7	3.00	2.29	149	171	178
					8	2.99	2.30	123	164	177
					10	2.91	2.16	143	142	150
					2	2.93	1.95	160	153	160
(7)	N_6—H··O_{14}=C_{38}		8NH→50	4→1	7	2.81	2.08	137	132	136
					8	2.82	1.89	133	135	134
					10	2.89	2.15	142	148	150
					2	2.86	2.00	141	139	140

[a] Alternative H-bond nomenclature used in ref 16. [b] Standard deviations in the distances between atoms are in the range of 0.01–0.02 Å for non-H atoms and in the range of 0.05–0.07 Å when one of the atoms is hydrogen. [c] Standard deviations in the angles are in the range of 0.5–1° for non-H atoms. [d] Author, please give footnoted.

and analogues later on in this paper.

Intramolecular Hydrogen Bonds in 7 and 8. The intramolecular hydrogen bonds (intraHB's) in the structures of **7** and **8** (along with the corresponding ones in **10** and **2**) are described in Table VIII. Only intraHB's of the N—H···O=X type for which the N···X distance is <3.2 Å, and for which the N–H···O angle is >105°, are considered. Of the seven observed intraHB's in amatoxin structures, five strong ones (No. 3–7 in Table VIII) of <3.00 Å are present in both **7** and **8**. These five bonds are shown (thin lines) in Figures 3 and 4. Since the structure and the intramolecular hydrogen bonding system of **7** and **8** are very similar, the different orientations of **7** and **8** in these figures provide essentially two different viewpoints of the common intramolecular arrangement.

The primary 24-membered ring is conformationally stabilized by two transannular intraHB's of the 5→1 and 4→1 types. The 5→1 intraHB (also called C_{13} or α-turn) between the Gly-5 NH group and the Asn-1 carbonyl group (No. 6 in Table VIII) holds together the bend consisting of residues 1–5 (most of ring 1) at one side of the molecule (top in Figure 3). The values of the backbone conformational angles of the central three residues of this turn (ϕ = −61° to −81°; ψ = −31° to −52°) are somewhat similar to those of the corresponding residues in right-handed α-helix (ϕ = −57°; ψ = −47°) and ω-helix (ϕ = −64°; ψ = −55°),[54,55] which are common secondary structures with 5→1 type repeating intraHB's. 5→1 intraHB's were also found in the structures of the cyclic decapeptide [Phe[4],Val[6]]-antamanide[56] and the cyclic dodecadepsipeptide valinomycin;[57,58] however, they consist of cis peptide bonds and therefore adopt different conformations.

The 4→1 intraHB between the Cys-8 NH group and the Gly-5 carbonyl group (No. 7 in Table VIII) holds together the bend of the other side of the molecule (bottom in Figure 3) consisting of residues 5–8 (part of ring 2). Four types of 4→1 intraHB's (also called C_{10} or β-turn) have been characterized[59] and observed[32,55,60,61] in folded peptide chains, and these are probably the most common of the secondary chain reversals (turns) in peptides and proteins. The 4→1 bond in **7** (and **8**), with conformational angles (ϕ,ψ) for the two central residues (6 and 7) of −63°, 134° and 79°, −2°, respectively (and similarly for **8**), belongs to the 4→1 trans II type (ϕ_2 = −60°, ψ_2 = 120°; ϕ_3 = 80°, ψ_3 = 0°)[59]. Similar 4→1 trans II intraHB's have been found in the structures of valinomycin,[57,58] the ferrichromes,[62a,b] and several other linear and cyclic peptides.[55]

Ring 1 is conformationally further reinforced in both **7** and **8** by three hydrogen bonds from main chain NH groups to side chain O=X groups (MC→SC intraHB's No. 3–5 in Table VIII). The Dihyile-3 NH group is hydrogen bonded to the Asn-1 side chain carbonyl group, forming (intraHB No. 4 in Table VIII) a 10-membered folded segment (C_{10} or β-turn like). The same carbonyl group is also hydrogen bonded to the next NH group (of residue 4) in the peptide backbone, forming a 13-membered folded segment (C_{13} or α-turn like). To the best of our knowledge, no such side chain–main chain interactions have been reported in crystal structures of oligopeptides (except of course for the other amatoxin structure of **10**);[17] however, similar interactions of an Asn β-C=O group with a main chain NH group (forming a C_{10}-like unit), and a Gln γ-C=O group with a main chain NH group (forming a C_{13}-like unit), have been suggested from solution NMR studies of oxytocin[21,63] and tocinamide,[21,64] respectively. Similar side chain–main chain interactions, resulting in β-turn like configu-

(54) Arnott, S.; Dover, S. D. *J. Mol. Biol.* **1967**, *30*, 209.
(55) Toniolo, C. *CRC Crit. Rev. Biochem.* **1980**, *9*, 1; and references therein.
(56) Karle, I. L. *J. Am. Chem. Soc.* **1977**, *99*, 5152.
(57) Karle, I. L. *J. Am. Chem. Soc.* **1975**, *97*, 4379.
(58) Smith, G. D.; Duax, W. L.; Langs, D. A.; DeTitta, G. T.; Edmonds, J. W.; Rohrer, D. C.; Weeks, C. M. *J. Am. Chem. Soc.* **1975**, *97*, 7242.
(59) Vankatachalam, C. M. *Biopolymers* **1968**, *6*, 1425.
(60) Smith, J. A.; Pease, L. G. *CRC Crit. Rev. Biochem.* **1980**, *8*, 315; and references therein.
(61) Karle, I. L. In *The Peptides*; Gross, E., Meienhofer, J., Eds.; Academic Press: New York, 1981; Vol. 4, pp 1–54 and references therein.
(62) Zalkin, A.; Forrester, J. D.; Templeton, D. H. *J. Am. Chem. Soc.* **1966**, *88*, 1810.
(63) Norrestam, R.; Stensland, B.; Brändén, C. I. *J. Mol. Biol.* **1975**, *99*, 501.
(64) Urry, D. W.; Walter, R. *Proc. Natl. Acad. Sci. U.S.A.* **1971**, *68*, 956.

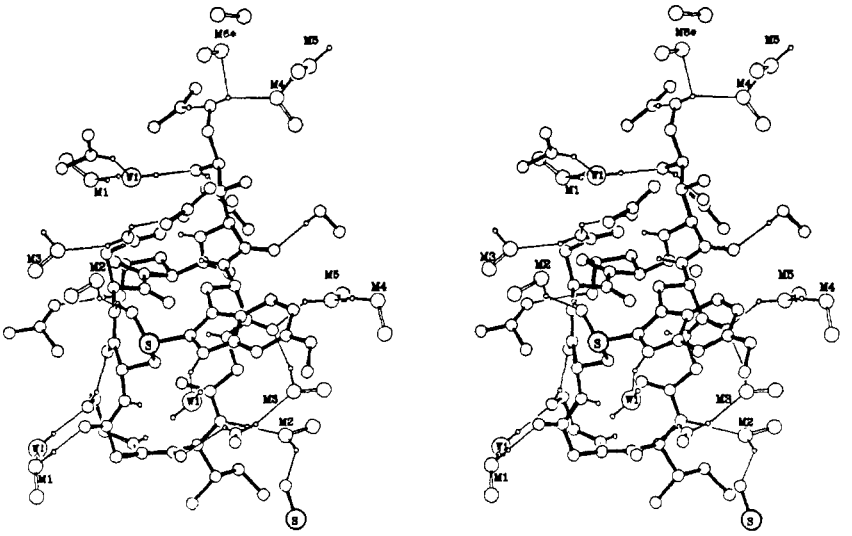

Figure 5. Solvent molecules, neighboring peptide regions, and intermolecular hydrogen bonds (thin lines) in the crystal structure of **7**. The cyclopeptide is outlined by solid lines, whereas interacting solvent molecules (large circles) and neighboring peptide regions (smaller circles) are designated by double lines.

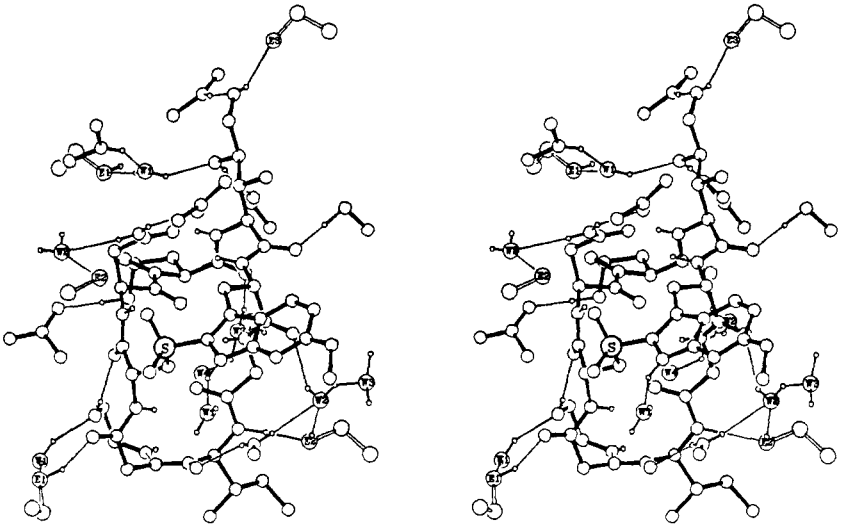

Figure 6. Solvent molecules, neighboring peptide regions, and intermolecular hydrogen bonds (thin lines) in the crystal structure of **8**. The cyclopeptide is outlined by solid lines, whereas interacting solvent molecules (large circles) and neighboring peptide regions (smaller circles) are designated by double lines.

rations, have been observed recently in the crystal structures of chymotrypsin, pancreatic trypsin inhibitor, and prealbumin,[31] and also in the 1.5 Å resolution structure of carboxypeptidase A.[65]

The third MC→SC interaction in ring 1 of **7** and **8** is a hydrogen bond between the Asn-1 backbone NH group and the (*S*)-sulfoxide group in **7**, or the (*S*)-oxygen (O1) of the sulfone group in **8**. This intraHB (No. 3 in Table VIII), forming a C_7-like (or γ-turn) hydrogen bonded ring structure, is unique to **7** and **8** and again, to the best of our knowledge, has not been observed before.

The system of strong intramolecular hydrogen bonds restrains the already firm bicyclic frame in **7** and **8**. The 18-membered ring of ring 1 seems especially "locked" in a very compact, essentially fixed conformation.

Intramolecular Hydrogen Bonds and Solvent Network in 7 and 8. The peptide–peptide intermolecular interactions are very similar in the crystal structures of **7** and **8**, resulting from similar crystal packing of the cyclopeptides in both crystal systems. However, although the molecular structure, the conformation, and the orientation in the crystallographic unit cells of **7** and **8** are almost identical, the solvent molecules and their arrangement in these two crystal structures are quite different. The coordinates of the solvent molecules and their numbering schemes in **7** and **8** are given in Tables III and IV, respectively. The intermolecular hydrogen-bonding networks in **7** and **8** are visualized in the stereo drawings of Figures 5 and 6, respectively. These intermolecular interactions are described in detail in Table IX, where the information on the related intermolecular networks in **10** and **2** is also given. In fully describing hydrogen-bonded networks, especially when large systems and water molecules are involved, one should note that there might exist more than one possible hydrogen-bonding scheme as long as not all the hydrogen atoms involved are located. Nonetheless, we are rather confident of the schemes described below, since most interacting hydrogen atoms have been uniquely located, and the geometries of the whole scheme and the individual groups involved are chemically reasonable.

Intermolecular Interactions in 7. Four peptide–peptide intermolecular hydrogen bonds (interHB's) are present in the crystal structure of **7**, all of which are interactions between side chain functional groups of one cyclopeptide and main chain carbonyl or NH groups of neighboring cyclopeptides (Table IX and Figure 5). One of the NH groups of the γ-NH_2 moiety of Asn-1 is hydrogen-bonded to a neighboring backbone carbonyl group of Ile-6 (3.04 Å). The γ-OH group of HyPro-2 is hydrogen-bonded

(65) Brewster, A. I.; Glasel, J. A.; Hruby, V. J. *Proc. Natl. Acad. Sci., U.S.A.* **1972**, *69*, 1470.

Table IX. Intermolecular Hydrogen Bonds[a] in 7, **8**, **10**, and **2**

	neighboring :Y group[c]							
	7		8		10		2	
peptide[b] X-H group	:Y	dist.[d]	:Y	dist.	:Y	dist.	:Y	dist.
N_1-H	OW1	2.86	OW1	2.85	OE2	3.05	$O_{11'}$	2.87
O_3-H							OW2	2.72
O_5-H	$O_{11'}$	2.76	$O_{11'}$	2.78			OW3	2.78
O_6-H	OM4	2.83	OE3	3.04			$O_{15'}$	2.73[e]
N_3-H	intra[f]		intra		intra		OW1	3.18
O_8-H	$O_{4'}$	2.79	$O_{4'}$	2.80	$O_{13'}$	2.75	OE2	3.00
N_{10}-H_1	OM3	2.99	OW2	3.13	OW2	2.92		
N_{10}-H_2	$O_{13'}$	3.04	$O_{13'}$	3.00				
O_{16}-H[g]							OE1	2.69
N_7-H	$O_{6'}$	2.97	$O_{6'}$	2.86	OW4	2.91	OE3	2.87
N_8-H	OM2	2.81	OE2	2.91	OW3	2.90	$O_{4'}$	2.88
	neighboring H-X group							
	7		8		10		2	
peptide Y: group	H-X	dist.	H-X	dist.	H-X	dist.	H-X	dist.
S=O_1[h]	H-OM2	2.79	H-OE2[i]	2.86				
S=O_2			H-$N_{1'}$[i]	2.82			H-OE2	2.79
O_3							H-OW1	2.70
C=O_4	H-$O_{8'}$	2.79	H-$O_{8'}$	2.80	H-OW4	2.68	H-$N_{8'}$	2.88
O_5	H-OW1	2.78	H-OW1	2.84			H-OW2	2.85
O_6	H-$N_{7'}$	2.97	H-$N_{7'}$	2.86			H-OW7a	3.20
	H-OM6	2.87					H-OW7b	3.06
C=O_7			H-OW3	2.92	H-OE1	2.76	H-OW5	3.03
					H-OW3	2.91		
C=O_{11}	H-$O_{5'}$	2.76	H-$O_{5'}$	2.78	H-OE2	2.82	H-$N_{1'}$	2.87
C=O_{12}	H-OM1	2.72	H-OE1	2.71	H-OW2	2.74	H-OW1	2.74
C=O_{13}	H-$N_{10'}$	3.04	H-$N_{10'}$	3.00	H-$O_{8'}$	2.75	H-OW3	2.94
							H-OE1	2.67
C=O_{15}	H-OM3	2.80	H-OW2	2.84			H-$O_{6(1)'}$	3.20[e]
	H-OM5	2.79					H-$O_{6(2)'}$	2.73

[a] H-bond of the type X-H···:Y, where the X···Y distance is less than 3.2 Å. [b] The numbering scheme presented in Figure 2 is used for all 4 cyclopeptides. [c] The numbering scheme for solvent molecules is taken from Tables III and IV for 7 and **8**, from ref 17 for **10**, and from ref 16 for **2**; W = water, M = methanol, and E = ethanol. [d] X···Y distance in Å; standard deviations are in the range of 0.005–0.015 Å. [e] Two of the three disordered positions of O_6 in **2** are located within hydrogen-bonding range from $O_{15'}$ with distances of 2.73 and 3.20 Å, respectively. [f] Participates in intramolecular H-bond. [g] O_{16}-H is the carboxylic OH group in **2**. [h] O_1 is the (*S*)-oxygen. [i] Questionable H-bond. The O-X distance compares well with the usual H-bond but the hydrogen position is off.

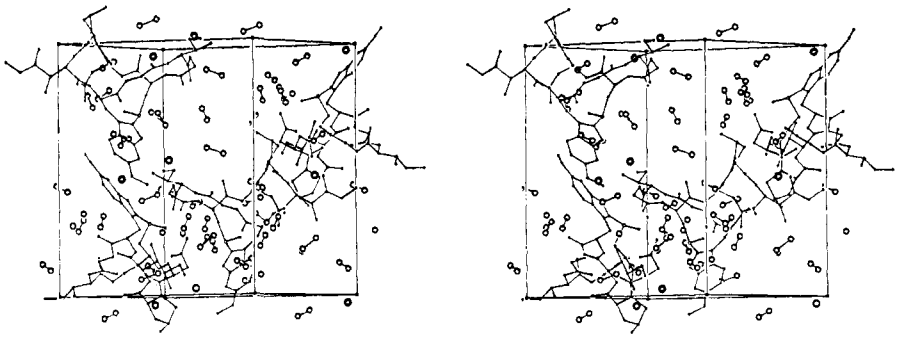

Figure 7. Stereodiagram of the unit cell packing of 7 in the crystal, viewed down the *a* axis (*c* axis vertical, *b* axis horizontal). Solvent molecules are represented by large circles where the water molecules are outlined in darker lines than the methanol molecules.

to a neighboring backbone carbonyl group of DihyIle-3 (2.79 Å). The γ-OH group of DihyIle-3 forms an interHB to a neighboring Cys-8 carbonyl (2.67 Å), whereas the oxygen atom of the δ-OH group of DihyIle-3 accepts an interHB from a neighboring NH group of Gly-7 (2.97 Å). It is interesting to note that of the six wide chain polar groups, four (X-H) groups are involved in interHB's and two (X=O) groups are involved in intraHB's; all six polar groups are located on ring 1 and all six hydrogen bonds are relatively strong.

Six methanol molecules (M1–M6) and a water molecule (W1) co-crystallize with **7** in the asymmetric unit. No attempts were made to completely dry the starting material or isolate the crystallization vial under dry nitrogen; thus it is not surprising to find water molecules in the crystal of **7**, obtained by crystallization from "pure" methanol.

All solvent molecules interact with the cyclopeptide (Table IX), and some of them (W1, M1, M4, and M5) interact among themselves (Table S11 of the supplementary material) to form a rather extensive hydrogen-bonded network (Figure 5). As a result, a few intramolecular and intermolecular "solvent bridges" are formed. An example of such an intramolecular bridge is the continuous hydrogen-bonded sequence of O13←H-N10′-H→-M3→O15 (where "→" represents the direction of the hydrogen bond), which links the backbone carbonyl groups of Ile-6 and MeOTrp-4, respectively, through a neighboring peptide side chain NH_2 group and a methanol molecule (Figure 5). Similarly, the sequence O12←M1←W1→O5′-H→O11 links the carbonyl groups of Gly-7 and Cys-8, respectively. Other intramolecular "solvent bridges" and intermolecular "solvent bridges" such as N1-H→W1→O5′, N8-H→M2→O=S′, and O6-H→M4→-M5→O15′ occur in the crystal of **7**, in varying length and complication of the hydrogen-bonded "chain".

Examination of the packing of the peptide and solvent molecules in the crystal (Figure 7) indicates that the molecules are grouped

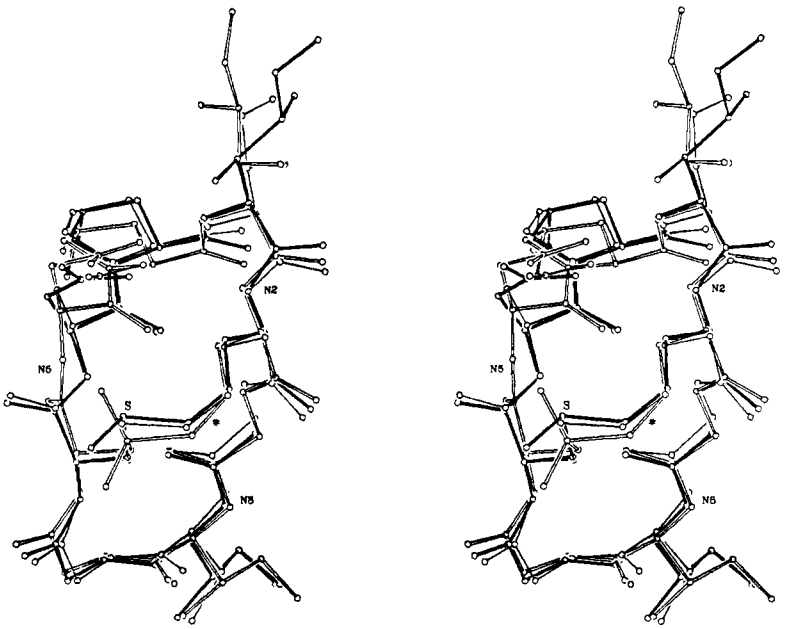

Figure 8. Stereoview of the crystal structure of β-Amanitin (**2**) (solid line) and the crystal structure of **8** (double line), superimposed, with the best RMS fit, on the crystal structure of **10** (thin line). The indole ring, located at the position designated by an asterisk, is omitted for clarity.

in continuous regions resulting in peptide "columns" and solvent "channels". The cyclopeptides interact with each other through hydrophobic contacts (e.g., the Ile-6 side chain with the Trp-4 indole ring) in addition to the interHB's described above. The solvent "channels" consist of both water and methanol molecules that are assembled along the *b* axis of the crystal.

Intermolecular Interactions in 8. The peptide–peptide intermolecular interactions in the crystal structure of **8** are almost identical with those described above for **7**. The small differences in the geometries of the four interHB's (Table IX) appear to be insignificant, and they are at least as strong as those of **7** (distances of 2.78–3.00 Å). An additional interHB, although weak, might exist between the ε-NH group of the indole ring and the (*R*)-oxygen (O2) of the sulfone group. Its distance is 2.82 Å; however, its geometry deviates substantially from that of an ideal linear bond.

Here again, the four water molecules and three ethanol solvent molecules co-crystallize in the asymmetric unit, forming part of a related, yet different, solvent–cyclopeptide hydrogen-bonded network (Table IX, Table S11, and Figure 6). Among the "solvent bridges" we will point out the chained hydrogen-bonded sequences of O13←H–N10′–H→W2→O15, N8–H→E2→W2→O15, and O12←E1←W1→O5′–H→O11, which link carbonyl and NH groups of the cyclopeptide backbone, and the hydrogen-bonded sequences of N1–H→W1→O5′ and O15←W2→W3→O7′, which link neighboring cyclopeptides. The packing of the peptide and solvent molecules in the crystal of **8** result in solvent "channels" (water and ethanol molecules) along the *b* axis (Figure S1 in supplementary material) similar to those described for **7**.

It is interesting to note that, with the exception of the HyPro-2 carbonyl group (O7) in **7**, virtually every possible group in **7** and **8** participates in an hydrogen bond, and some in even more than one; several groups form bifurcated hydrogen bonds (e.g. $C{=}O_{10}$ and $C{=}O_{15}$). The "solvent bridges" and the extensive hydrogen-bonded network described, part of which is probably preserved in solution and in the amatoxin–enzyme complex in vivo, provide an additional conformational stability and comparative rigidity to the amatoxin molecules.

Discussion

The crystallographic results presented above clearly indicate that the three-dimensional structures of the amatoxin derivatives **7** and **8** are almost identical. It is also apparent (Tables V–IX) that the structures of all four amatoxins now determined are generally similar. Yet, the four derivatives exhibit significantly different in vitro and in vivo biological activity (Table I). In an effort to determine which specific structural or chemical factor(s) is/are responsible for the observed differences, we compare in detail the four crystal structures. It should be noted that since the amatoxins bind very strongly to RNA polymerase B ($K_i \approx 10^{-8}$ M) the binding is expected to consist of more than a single intermolecular interaction and the contact is expected to be relatively tight. Therefore even a small relative mislocation of an interacting group (or non-interacting group, for that matter) in the amatoxin molecule could be the cause of a substantial reduction in activity. For convenience and consistency with previous sections we examine the structures according to backbone, side chains, sulfur bridge, hydrogen bonds, and overall appearance; also solvent interactions and crystal packing effects are discussed. Hopefully this comparison might indicate some general structure–activity relationships in the amatoxin series. Additionally, since we are dealing with a unique bicyclic system and unusual amino acid composition, we relate the observed structural parameters to conventional ones in polypeptide structures and discuss unusual features.

The four amatoxin structures have been compared by least-squares rotation methods.[66] A schematic representation of this comparison is shown in Figure 8, where the crystal structures of **2**, **8**, and **10** are superimposed after least-squares fitting **8** to **2**, and **10** to **2** (in which uncommon atoms and the atoms of side chain 3 where ignored). Since the structure of **7** appeared to be in nearly complete overlap with that of **8**, only the structure of the latter was included in Figure 8 for clarity. A similar fit of the sulfur-containing bridge in the amatoxin structures is presented in Figure 9.

Peptide Backbone Structure in the Four Amatoxin Derivatives. The geometry of the peptide bond and the specific bond lengths and bond angles in polypeptide chains have been shown to be essentially invariant among linear peptides, simple cyclopeptides, and proteins.[22-27] Bond lengths and bond angles of the peptide backbone generally compare well among the four amatoxin derivatives, and all agree rather well with the corresponding parameters commonly observed in peptides and proteins (Tables S7 and S8). The values for both bond lengths and bond angles in **2** deviate somewhat from the mean and the corresponding values in the other three derivatives; however, we relate the differences to the lower degree of accuracy in the crystal structure determination of **2**[16] (lower resolution of data and higher agreement factor than for the other three) rather than to any significant trend.

In fact, the mean values for the specific distances and angles in the backbones of all four derivatives compare favorably with all "standard" peptide unit geometries reported in the past[22-27]

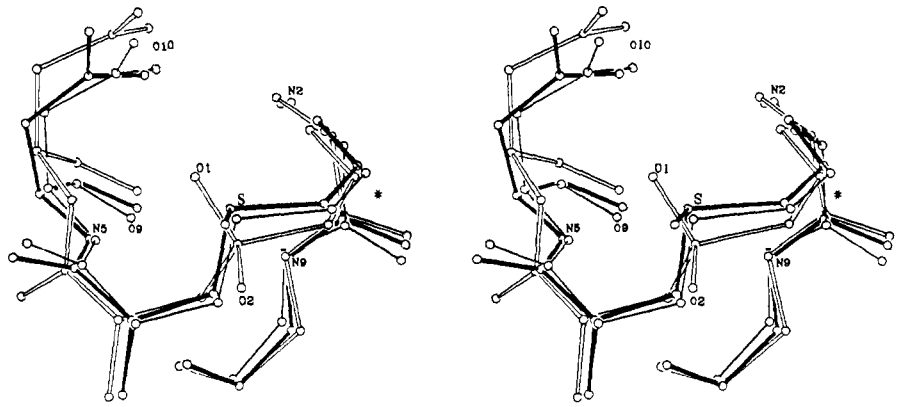

Figure 9. Comparison (best RMS fit) of the sulfur bridge in the crystal structures of **2** (solid line), **8** (double line), and **10** (thin line), respectively. The structure of **10** was intentionally translated (by 0.2 Å) from the best RMS fit position (by 0.2 Å) to the lower right corner of the drawing, for clarity (since it overlapped for the most part with **2**). Similarly, the indole ring (designed by an asterisk) was omitted.

and are almost identical (the differences are ≤0.006 Å and ≤0.9°, respectively) with the mean values calculated for 34 simple peptides[25] (Tables S7 and S8). Considerable deviations around the mean value (112.0°) are noticed in the τ angle (N_i–C_i^α–C_i) of the different residues, especially Pro and Gly; however, among the four derivatives the corresponding angles of the specific amino acids are very similar. Some flexibility of the τ angle has been observed in other polypeptide systems and proteins (e.g., ref 67 and 68), and $\tau > 112°$ is usually attributed to accommodation of some strain in the structure;[31] in particular, larger τ angles are commonly observed for Gly residues.[24]

As for the planarity of the peptide unit (ω) and the angular relations between peptide units (ϕ,ψ), no unusual values are found for all four amatoxins (Table V). All ω angles[28] are within 180 ± 14° and the mean for all four polypeptide chains is −178°, which agrees well with the most stable trans conformation (ω = 180°). Nevertheless, noticeable deviations from planarity occur at residues 3, 4, 7, and 8. These nonplanar deformations of the peptide bond are probably due to some strain on the backbone caused by the uncommon bridge between the side chains of residues 4 and 8. However, the strain is not likely to be significant, since nonplanar distortions of that magnitude are not unusual[25,32,67,68] and out-of-plane deformations can be made at very modest energy cost[32-34] as indicated above.

All backbone torsion angles fall within the allowed regions of the ϕ,ψ plot.[29] The "α-helical" segment of residues 2, 3, and 4 and the β-turn part of residues 5–8, described above for **7** and **8**, are similar in **10** and **2** (Table V, Figure 8), although with small differences in the ϕ,ψ values of residues 3 and 4 and a larger difference of the ϕ value of residue 5 in **10**. However, the primary difference in the backbone conformations of the four amatoxins lies at the peptide bond between residues Cys-8 and Asn-1. The plane of this peptide bond, which is generally parallel to the plane of the ring 1 backbone in **10** and **2** (Figures 8 and 9), is almost perpendicular to the ring 1 plane in **7** and **8**. This 90° rotation of the peptide plane brings the carbonyl group of Cys-8 outward and the NH group of Asn-1 inward, in **7** and **8**. In addition to the ≈100° change in the values of ψ_8 and ϕ_1, this twist causes ≈20° change in ψ_1 and considerable translation in the relative position of the Asn-1 residue (Figure 8). The ϕ_1,ψ_1 conformation lies within the allowed "β" region of a Ramachandran plot[29] in both orientations of the peptide plane, whereas the ϕ_8,ψ_8 conformations lie within the "α" region in **10** and **2** and in the "β" region in **7** and **8**. This implies a considerable energy barrier for the above rotation (crossing an unallowed region in a Ramachandran plot,[29] or C_i^β–H_{i+1} sterical constrain (clashing),[30] upon rotation), although τ angles that deviate from 110° and ω angles that deviate from 180° provide more flexibility (or extension of the allowed region) for the peptide backbone conformation.[31-33] The 90° rotation of the peptide unit in **7** and **8** is probably driven by the formation of a new strong intraHB between N5–H and O1=S; the sulfoxide (*S*)-oxygen (O1), of course, is not present in **2** or **10**.

Least-squares fit[66] of the 24-membered cyclopeptide backbone in the four structures gives RMS deviations[69] of 0.54, 0.56, 0.31, 0.07, 0.63, and 0.64 Å between the backbone atoms of **2** vs **7**, **2** vs **8**, **2** vs **10**, **7** vs **8**, **7** vs **10**, and **8** vs **10**, respectively. This comparison again shows that, on the average, the amatoxin peptide backbone adopts similar overall conformations. However, while the backbones of **7** and **8** are practically identical, they differ locally from the backbones in **2** and **10**; in addition to the twist and displacement of the backbone 6-membered segment C27–C19 (Asn-1 and HyPro-2), as described above, noticeable deviations occur at the carbonyl groups of residue-3 (O4) and residue-4 (O15) (Figure 8). The backbones of **2** and **10**, although better correlated to each other than to **7** or **8**, exhibit small local deviations in the orientation of the carbonyl groups of residues 2, 3, 4, and 6 (O7, O4, O15, and O13, respectively), and to lesser extent in the relative position of Gly-5 C^α (Figure 8).

Nevertheless, despite all of the small differences described above, the backbone structures of the four amatoxin derivatives are, for the most part, similar. Likewise, despite some deviations of structural parameters from the commonly observed values, the backbones of the four amatoxin derivatives do not seem to experience any major local or ring strain.

Side-Chain Conformations in the Four Derivatives. Bond lengths and bond angles in the side chains of all four amatoxin derivatives[16,17] are similar and in general they agree well with the usually observed corresponding parameters in the side chains of single amino acids and small peptides in crystal structures[35,36] (Tables S9 and S10). The few small deviations that occur in these parameters (e.g. the bond distances of C17–O6 in **2**, C16–C17 in **10**, and C36–C37 in **7**) are probably due to relatively large thermal motions or local disorders in the crystal, especially in the side chains of the two isoleucine residues.

The conformations of side chains are nearly identical in **7** and **8**; however, there are some differences in **2** and **10**, with the exception of the Ile-6 side chain which adopts a similar conformation in all four structures (Table VI and Figure 8). The Asn-1 side chain in **7** and **8** is displaced by about 0.6 Å from the average plane of ring 1, in comparison to **2** and **10**, due to the twist in the peptide backbone described above. In addition, the plane of the terminal amide group of Asn-1 in **7** and **8** is rotated by ≈40° from its corresponding (carboxylic group) more stable[42] orientation in **2** ($\chi^2 \approx 20°$); the orientation of the amide group in **10** is between these two. As a result the position of the $COOH/CONH_2$ group relative to the rest of the molecule is different in the three cases (**2**; **7** and **8**; **10**), affecting the intramolecular hydrogen bonds between C=O10 and the peptide backbone (one of the intraHB's

(66) (a) Kabsch, *Acta Crystallogr.* **1976**, *A32*, 922. (b) Kabsch, W. *Ibid.* **1978**, *A34*, 827.
(67) Deisenhofer, J.; Steigemann, W. *Acta Crystallogr.* **1975**, *B31*, 238.
(68) Watenpaugh, K. D.; Sieker, L. C.; Jensen, L. H. *J. Mol. Biol.* **1979**, *131*, 509.
(69) Root-mean-squares deviation in the position of related common atoms in two compared structures.

is missing in **2**, as discussed below).

The hydroxyproline ring of residue 2 assumes the same puckered conformation (C_s–C^γ–exo[44]), and the γ-OH group is displaced by approximately 2 Å perpendicular to the proline ring plane in all four derivatives. Yet, here again, because of the "twist" in the peptide backbone in this region, the proline ring and more importantly the γ-OH group lie in a somewhat different orientation relative to the rest of the molecule in **7** and **8** vs **2** and **10** (Figure 8).

A major difference in side chain conformation is seen in residue 3 (Figure 8). In **7**, **8**, and **10** the two C^γ atoms lie close to the preferred spatial position ($\chi^{1,1} \approx -60°$, $\chi^{1,2} \approx 180°$;[42,70] see discussion above), where in **2** they lie in different positions, slightly away from the less favored conformation where $\chi^{1,1} \approx -180°$ and $\chi^{1,2} = 60°$. In addition to intermolecular interactions in the crystals, this ≈70° rotation around the C^α–C^β bond (in **2**) could be due to the interference of the β-methyl group with the adjacent carbonyl oxygen (O4), which is differently oriented in **2** (Figure 8). The C^δ atoms in **7**, **8**, and **2** (which are close to the *t* conformation) and the substituted OH groups (O5 and O6 in **7**, **8**, and **2**) assume a stable staggered conformation. Since the C^δ atom (C17) of Ile-3 in **10** is considerably disordered, it is difficult to evaluate the different $\chi^{2,2}$ value observed (Table VI); in fact this is the conformation of only the most populated rotamer and the other disordered positions result in the $\chi^{2,2}$ range of −20° to 60°. Nonetheless, in all these possible orientations of C^δ, the terminal methyl group in **10** occupies the approximate space occupied by the γ-OH group in the other derivatives. The detailed conformation of side chain 3 is of great interest because it has been shown that small chemical modifications in this side chain result in significant reduction of the biological activity of amatoxins.[7,13] It is important to note that a relatively low rotational barrier of ≈2 kcal/mol[36] is expected around the C^α–C^β and the C^β–$C^{\gamma,1}$ bonds in the Ile side chain; however, the rotational barrier around C^α–C^β is sensitive to the local backbone conformation and barriers of 1–5 kcal/mol are possible in specific ϕ,ψ settings.[43,71] The above indicates that although the DihyIle-3 side chain in **2** is rotated by ≈70° from the more stable conformation in **7**, **8**, and **10** (resulting in different relative positions and orientation of the critical OH groups), the energy difference between these two conformations is not necessarily significant. It should be noted that the conformation of the Ile-6 side chain in all four derivatives agrees well with the most favorable conformation[42,43,71] (i.e. $\chi^{1,1} \approx -60°$, $\chi^{1,2} \approx 180°$, and $\chi^2 \approx 180°$).

The tryptophan side chain assumes a very similar conformation in all four amatoxins (Figures 7 and 8 in ref 17), despite the different substituents at the indole ring 6′ position and the different nature of the sulfur-containing bridging group (at the indole group 2′ position). The χ^1 and χ^2 values are away from the preferred setting[42] of −60° and ±90°, respectively, which is not unexpected given the location of the transannular bridge (especially the deviation from the usually observed[40-42] $\chi^2 \approx \pm 90°$). No significant deviation from planarity of the indole ring is observed in any of the derivatives and this plane practially overlaps in all four (Figures 7 and 8 in ref 17).

The Sulfur-Containing Bridge. The chemical character of the bridging sulfur group has been shown to be important for the biological activity of amatoxins.[7,13] The (*S*)-sulfoxide bridging group especially exhibits significant reduction in binding affinity to RNA polymerase B and a more dramatic decrease in toxicity, in comparison with the other bridging sulfur groups. The four amatoxins discussed here contain a thioether (**10**), an (*R*)-sulfoxide (**2**), an (*S*)-sulfoxide (**7**), and a sulfone group (**8**) as bridging units, providing a complete set for the examination of the structural role of the sulfur-containing bridge.

A detailed comparison of the geometrical parameters of the bridging unit in **7**, **8**, **10**, and **2** is presented in Table VII. Also listed in Table VII are the analogous parameters of similar units in two model compounds, a simple synthetic monocyclic peptide (12-membered macrocycle) and an indole–thioether unit[46] (model compound 1 or Mod-1) and a derivative of L-tryptophane (acyclic) with an indole–(*R*)-sulfoxide unit[47] (model compound 2 or Mod-2).

On the average the C–S bond in the amatoxins is slightly shorter than the usual single C–S bond;[38] however, the C–S bond lengths in the amatoxins compare well with the corresponding values in the structure of dimethylsulfoxide[48-50] (DMSO; 1.77–1.82 Å), dimethyl sulfone[51-53] ($DMSO_2$; 1.76–1.78 Å), and dimethyl sulfide[72] (DMS; 1.81 Å). The C1–S bond is significantly shorter than the C29–S bond, probably due to the different hybridization of these two carbon atoms (sp^2 for C1 and sp^3 for C29); a similar effect occurs in the two model compounds. As expected the S–O bond is shorter in the sulfone group in **8** than in the sulfoxide groups (in **2** and **7**); this result is consistent with the parameters of the corresponding small molecules.[38,48-53,72] Also, as observed in small molecules,[48-53,72] the C–S–C bond angle is considerably larger for the sulfone (**8**) than for the sulfoxides (**2** and **7**) or the sulfide (**10**).

Since the bond lengths and bond angles of the sulfur group in the four amatoxin derivatives are similar to those in the related DMS, DMSO, and $DMSO_2$ structures, one would expect to find corresponding similar dipole moments in the two sets; the measured (molecular) dipole moments (μ's) for DMS, DMSO, and $DMSO_2$ are 1.50,[73] 3.96,[48] and 4.43 D,[52] respectively. These molecular dipole moments are consistent with the assumption of similar individual bond moments in these three molecules, that is 1.47 D for the C–S bond and 2.70 D for the S–O bond.[52]

An ab initio molecular orbital analysis (PRDDO)[74,75] at the minimum basis set level has been performed in our laboratory on models of the indole–sulfoxide and indole–sulfone units, using the crystallographic coordinates of **7** and **8**, respectively. This study further indicates that the individual S–O bond dipole moments of the sulfoxide and sulfone are similar also in the larger systems of **7** and **8**. Furthermore, charge distribution analyses (Armstrong, Perkins, and Stewart[76] or Mulliken[77] electronic population analyses) of these two systems indicate that the partial charge on the oxygens is similar in both the sulfoxide and the sulfone moieties. The detailed analysis of dipole moments and charge distribution is important for the understanding of the structure–activity relationships in amatoxins discussed below.

In contrast to the similar bond lengths and bond angles, the conformation of the sulfur bridge is somewhat different among the four amatoxins, especially in comparing **7** and **8** vs **2** and **10** (Table VII, section 3, and Figure 8). The sulfoxide/sulfone group in **7** and **8** is rotated by ≈40° around the general axis of the bridge, away from the rest of ring 1, relative to the position of the analogous group in **2** and **10**. This modified conformation in **7** and **8** could result from the altered backbone conformation at the Cys-8–Asp-1 linkage (the 90° "flip") and some van der Waals repulsion of the (*S*)-oxygen from adjacent groups in ring 1 (e.g. Asn-1 side chain and Trp-4 β-methylene group). This local rotation also allows for a better hydrogen-bonding geometry between the N5–H and O1=S groups (Figure 8). The net result of this slight twist in the transannular bridge is that the sulfur atom in **7** and **8** is displaced by ≈0.5 Å relative to its spatial position in **2** and **10**, and that the (*R*)-oxygen of **8** is displaced by ≈1 Å relative to its spatial position in **2** (and also lies in slightly different orientation). Not surprisingly (due to the bridging effect) the Cys-8 χ^1 torsion angle in all four amatoxins deviates significantly from the preferred g^+ conformation ($\chi^1 \approx 60°$),[42] which is demonstrated in the case of the more relaxed system of Mod-1. A

(70) The most favorable conformation ($\chi^{1,1} \approx -60°$; $\chi^{1,2} \approx 180°$; $\chi^2 \approx 180°$) was computed and observed for an isoleucine residue; however, no qualitatively different values are expected for the substituted Dihylle residue.

(71) Lewis, P. N.; Momany, F. A.; Scheraga, H. A. *Isr. J. Chem.* **1973**, *11*, 121.

(72) Iijima, T.; Tsuchiya, S.; Kimura, M. *Bull. Chem. Soc. Jpn.* **1977**, *50*, 2564.

(73) Pierce, L.; Hayashi, M. *J. Chem. Phys.* **1961**, *35*, 479.

(74) Halgren, T. A.; Lipscomb, W. N. *J. Chem. Phys.* **1973**, *58*, 1569.

(75) Marynick, D. S.; Lipscomb, W. N. *Proc. Natl. Acad. Sci., U.S.A.* **1982**, *79*, 1341.

(76) Armstrong, D. R.; Perkins, P. G.; Stewart, J. J. P. *J. Chem. Soc., Dalton Trans.* **1973**, 838.

(77) Mulliken, R. S. *J. Chem. Phys.* **1955**, *23*, 1833.

comparison of the bridge torsional angles to the corresponding ones in Mod-1, however, indicates that the general bridge conformation in **2** and **10** is exposed to somewhat less strain than in **7** and **8**.

With regard to the overall similarities in side chain geometries in the four amatoxins, it is interesting to find that a least-squares fit[66] of the non-backbone atoms (including the bridging segment) in the four structures gives RMS deviations[69] of 0.64, 0.67, 0.60, 0.11, 0.51, and 0.52 Å, between the side chain atoms of **2** vs **7**, **2** vs **8**, **2** vs **10**, **7** vs **8**, **7** vs **10**, and **8** vs **10**, respectively. These figures show that except for the high similarity between the side chain conformations of **7** and **8**, no other pair among the four derivatives shows significantly unique side chain similarities.

Least-squares fit[66] of all 58 common atoms in the four amatoxin structures (excluding C17 which is disordered in **10**) gives RMS deviations[69] of 0.60, 0.63, 0.48, 0.10, 0.60, and 0.61 Å for **2** vs **7**, **2** vs **8**, **2** vs **10**, **7** vs **8**, **7** vs **10**, and **8** vs **10**, respectively, confirming again that the structures of **7** and **8** are practically identical, whereas the overall structures of **2** and **10** are only slightly more similar to each other than to **7** or **8**. The superposition of the amatoxin structures shown in Figure 8 is the result of the overall least-squares fit described above.

Intramolecular Hydrogen Bonds. Seven types of intraHB's have been observed among the four amatoxin structures (Table VIII), some of which are unique. Four intraHB's are between backbone groups only: a 2→2 intraHB between the NH and C=O groups of Asp/Asn-1 (intraHB No. 1 in Table VIII), a 4→1 intraHB between the Cys-8 NH group and Gly-5 C=O group (intraHB No. 7), a 5→1 intraHB between the Asp/Asn-1 NH group and the Gly-5 C=O group (intraHB No. 2), and another 5→1 intraHB between the Gly-5 NH group and the Asp/Asn-1 C=O group (intraHB No. 6). Additionally, three intraHB's occur between the backbone NH groups of DihyIle/Ile-3 and Trp-4 and the side chain carbonyl of Asp/Asn-1 (intraHB's 4 and 5, respectively), and between the Asp/Asn-1 backbone NH group and the bridging S=O1 group (intraHB No. 3). While intraHB's 5–7 are observed in all four amatoxin structures, intraHB 4 is observed only in **7**, **8**, and **10**, intraHB 3 is observed only in **7** and **8**, and intraHB's 1 and 2 are observed only in **2** and **10** (Table VIII). Obviously, due to geometrical constraints, intraHB's 1, 2, and 3 cannot occur simultaneously in these systems.

A 2→2 intraHB (or C_5 conformation) is possibly only at the fully extended backbone conformation[78] and was demonstrated to represent a real, although weak, intramolecular interaction.[78] The 2→2 intraHB's have been theoretically considered (e.g. ref 71) and experimentally observed in linear peptides,[32,55,78] mainly in glycyl residues, and are characterized by typical values of ≈2.60 and 2.15 Å for the N···O and H···O distances, respectively. The 2→2 intraHB in **2** and **10** exhibit similar distances, and the interactions apparently contribute to the stability of backbone ring 1 (Figure 4 in ref 17).

The 4→1 type II all-trans[59] intraHB, found in all four structures, is a fairly common folded conformation in polypeptide chains,[60] especially when the central residues of the turn (ref 2 and 3) are L-D, D-L, Gly-L, or L-Gly sequences;[61] the latter is the case in amatoxins. The ϕ,ψ values of these central residues in the four amatoxin structures (Ile-6 and Gly-7) are similar (Table 5) and compare well with the ideal theoretical values calculated for this type of turn.[59] In all four structures the hydrogen bonding distance is <2.9 Å, indicating a strong interaction and essential stabilization of backbone ring 2.

The 5→1 intraHB is a less-common[56-58] folded structure in cyclic peptides. There is more conformational flexibility in this larger turn than in the other polypeptide turns, and indeed the conformations of the two such 5→1 structures found in amatoxins are considerably different. One of the 5→1 intraHB's (No. 6), observed in all 4 structures, forms a "helical" fold consisting of residues 2, 3, and 4, as discussed above. The backbone ϕ,ψ values of the central residues of this turn in the four amatoxins are generally similar, yet not as conserved as in the 4→1 structure (Table V). This 5→1 HB is also a relatively strong intraHB (<3.0 Å) and appears to be essential for the stability of the primary macrocycle. The other 5→1 intraHB (No. 2), observed only in **2** and **10**, forms a relatively "flat" fold[16,17] consisting of residues 6, 7, and 8 and is considerably weaker (hydrogen-bonding distance ≈ 3.15 Å).

All three hydrogen-bonding interactions between side chain and backbone groups found in the amatoxin structures are unique to this system. However, it is interesting to note that the size of the cyclic structure being formed by these intraHB's compares well with known backbone turns, namely 7-, 10-, and 13-membered folded conformations for intraHB's 3, 4, and 5, respectively. The N5–H→O1=S intraHB (No. 3) observed only in **7** and **8** is relatively strong and provides considerable rigidity to ring 1 and the whole bicyclic frame. It is probably the formation of this bond that drives the rotation of the peptide unit between residues 8 and 1. This rotation, in turn, prevents the preservation of the 2→2 and the 5→1 (No. 2) intraHB's observed only in **2** and **10**, as discussed above. Yet the "trade" of intraHB's 1 and 2 for intraHB 3 in **7** and **8** is probably energetically favored, since both intraHB's 1 and 2 are relatively weak as mentioned above.

The two intraHB's formed by the interaction of the carbonyl group of side chain 1 with two backbone NH groups (intraHB's No. 4 and 5) provide a good example of the intramolecular hydrogen-bonding capability of the carboxylic and amide side chains. Although chemically sound, these types of interactions have been considered or reported quite rarely in oligopeptide structures (and only very recently in protein structures[31,65]). Surprisingly few such hydrogen bonds have been suggested from solution work with peptides,[64,65] as mentioned above, and a related 7-membered-ring structure has been found in the crystal structure of the linear peptide Piv-L-Gln-NHMe.[79] The two intraHB's serve both to stabilize the backbone of ring 1 and to fix the Asp/Asn side chain in compact conformation close to the peptide main chain. These two intraHB's are relatively strong (<3.0 Å) in **7**, **8**, and **10**, whereas in **2** some differences in the peptide backbone and the conformation of the side chain (see above) result in a geometry in which only one of these interactions (intraHB No. 5) takes place, and is weak (d = 3.15 Å); the other N···O distance is too long (d > 3.30 Å) to be significant.

The intramolecular side chain–main chain hydrogen bonds are important not only for the stabilization of the backbone and the side chain conformations but also for the "deactivation" of the functional groups of side chains, preventing them from participating in intermolecular interactions (e.g. with functional groups of the binding enzyme).

It is very interesting to note the multicenter hydrogen bonds and the intramolecular network created in the four amanitin structures. In **2** and **10** both O9 and O14 participate in two simultaneous intraHB's (acceptor bifurcated hydrogen bonding), and similarly the N5–H group participates in two simultaneous intraHB's (donor bifurcated hydrogen bonding or three-center hydrogen bond[80,81]). In the same way O10 (of the Asn side chain) in **7**, **8**, and **10** participates in acceptor bifurcated hydrogen bonding as described above. Two of the acceptor bifurcated H bonds (involving O14 and O10) result in "overlapping" folded units (or loops), namely a C_{10} structure contained within a C_{13} structure, which we represent as (C_{13}(C_{10})) or 5→(4→)1;[82] the third acceptor bifurcated H bond results in "fused" units, namely a C_5 structure sharing a bond (C=O) with a C_{13} structure, which we represent as ((C_5)(C_{13})) or 1→1←5. The donor bifurcated H bond analogously results in "fused" (N–H bond sharing) C_{13} and C_5 structures, which we represent as ((C_{13})(C_5)) or 1←5→5. Moreover, some of these combined hydrogen-bonded units occur

(78) Toniolo, C. In *Bioorganic Chemistry*; van Tamelen, E. E., Ed.; Academic Press: New York, 1977; Vol. 3, pp 265–291.

(79) Aubry, A.; Protas, J.; Marraud, M. *Acta Crystallogr.* **1977**, *B33*, 2534.

(80) Jeffrey, G. A.; Maluszynska, H. *Int. J. Biol. Macromol.* **1982**, *4*, 173.

(81) Taylor, R.; Kennard, O.; Versichel, W. *J. Am. Chem. Soc.* **1984**, *106*, 244.

(82) The notations 5→(4→1)1 and 5→1←4 and could both be used similar; however, the former representation seems clearer.

consecutively along the peptide backbone in **2** and **10**, forming a "mini network" or "zig-zag linkage" across the primary 24-membered macrocycle (Figure 4 in ref 17), which likely provides additional stability and rigidity to the overall conformation of the molecule. According to the representation outlined above, this integrated hydrogen-bonding system could be written down as 9→5←5→(4→)1 (where 9 and 1 are the same amino acid in our cyclic peptides).

Although relatively common in organic crystal structures[81,83,84] and proteins,[85] intramolecular bifurcated hydrogen bonds are rarely reported for oligopeptides, especially for cyclopeptides. Spectroscopic results in solution suggested the existence of a 3←3→1 or $((C_5)(C_7))$ H-bonding system in the protected dipeptide Bu^{t}CO-L-Pro-Aib-NHMe,[86] and the existence of a 4←4→1 (or $((C_5)(C_{10}))$ H-bonding system in the protected tridepsipeptide Ac-D-Val-L-Lac-L-Val-OMe.[87] A 5→(4→)1 (or $(C_{13}(C_{10}))$ H-bonding system, similar to that in **2** and **10**, has been described in the crystal structure of the antibiotic cyclohexapeptide ilamycin B_1[88] (although containing a cis peptide bond) and recently was observed in the crystal structures of the linear protected hexapeptide Boc-(D-aIle-L-Ile)$_3$-OMe[89] (with ϕ,ψ values very similar to those in **2** and **10**) and the linear protected dipeptide Boc-D-Leu-L-Phe-EA[90] (which contains an oxy analogue of C_{13}).

Regarding the geometry of the intraHB's in the four amatoxin structures it is noted that most N—H···O and H···O=C angles deviate significantly from linearity (Table VIII). However, it was shown statistically that N—H···O angles are rarely equal to 180°,[83,84,91] and that H···O=C angles tend to correlate more with the oxygen sp^2 lone pairs (mean of ≈130°);[91] the deviations of the hydrogen bonds from optimal geometry are shown to be more pronounced in multicenter hydrogen bonds.[81] The observation that in general the H···O=C angle deviates from 120° less than the N···O=C angle (Table VIII) indicates that the N–H group prefers to point "toward" the idealized lone pair, as has been previously suggested,[91] rather than "away" from it. Related aspects of the directionality of the lone pair in hydrogen bonds are discussed elsewhere.[92]

Intermolecular Hydrogen Bonds and Crystal Packing. As is apparent from Table IX, all four amatoxin crystal structures exhibit extensive intermolecular hydrogen-bonding systems and especially interactions between the cyclopeptides and the surrounding solvent molecules. In fact, with the exception of the C=O7 group in **7** and the C=O15 and N10—H2 groups in **10**, all of the potential H-bonding groups participate in at least one hydrogen bond. Moreover, examination of the crystal packing of **7** (Figure 7) and **10**[17] (see also supplementary material) indicates that these three exceptional groups are partially blocked by intermolecular contacts rather than intramolecular factors (although C=O15 in **10** is slightly hindered by the indole ring; Figure 6 in ref 17). The above findings are very important, suggesting that all polar groups that are not participating in intramolecular hydrogen bonding in the amatoxin molecules are potential candidates for intermolecular hydrogen bonding and therefore should be considered for possible binding interactions with the RNA polymerase B enzyme (before further structure–activity considerations).

We also note that the sulfide sulfur in **10** is not involved in any intermolecular (or intramolecular) interactions, although relatively exposed to the solvent region; the closest neighboring peptide atom is more than 4 Å away. Participation of sulfur atoms in hydrogen bonding has been reported in the iron–sulfur proteins (e.g. ref 93) and small peptides (e.g. ref 94), yet these interactions are generally rare. Thus with the support of the crystal structure we suggest that it is unlikely that the sulfide sulfur in **10** participates as a receptor for hydrogen-bonding interaction with the enzyme, in correlation with the activity role of the sulfur group in amanitin as discussed below.

It is interesting to note that the γ-OH group of DihyIle-3 in **2**, **7**, and **8** (O5-H), which has been shown to be important for inhibition and toxicity,[7,13] acts both as H-bond donor and H-bond acceptor. Both interHB's are relatively strong ($d < 2.85$ Å), and in all three structures the corresponding H-bond donor is a water molecule in full occupancy and low thermal factor. Similarly, the γ-OH group of HyPro in all four amatoxins, shown to be very critical for biological activity, participates only as a hydrogen donor in a fairly strong interHB (2.75–3.00 Å). These points are considered below in relationship to the amatoxin activity.

Although the detailed solvent arrangement and the specific intermolecular interactions in the crystals are different (among the four structures), a similar general pattern is noted. In all four amatoxins the cyclopeptides interact with each other, in addition to the interHB's, through hydrophobic groups (Ile-6 with backbone in **2**, Ile-6 with Trp-4 in **7** and **8**, and Ile-6 with Ile-6′ in **10**) resulting in continuous hydrophobic regions inaccessible to solvent. Solvent molecules generally form "channels" running between these regions and interact with the cyclopeptide polar groups and among themselves (Figure 7 and Figures S1, S2 and S3). The solvent "channels" provide somewhat easier translocation of solvent molecules within the crystal. Considering the important interconnecting role of the solvent molecules these "channels" could account for the relatively fast drying that leads to deterioration of the amatoxin crystals upon exposure to the air.

The Conformation of Amatoxins in Solution. Early CD and ORD investigations[15] suggested that the biologically active natural amatoxins (e.g. compounds **1** – **3**), as well as the less active amatoxins **4** (amanullin) and **12**, assume similar conformations in aqueous solution. Furthermore, these studies indicated that the observed common conformation of the amatoxins does not change significantly in organic solvents such as methanol or acetonitrile, yet they suggested some degree of conformational change in DMSO. A different conformation was also suggested[15] for the inactive Aldoamanitin derivative **11**. NMR studies[95] demonstrated that the conformation of α-amanitin (**1**) in DMSO solution is similar to that of β-amanitin (**2**) in the crystalline state[16] (crystallized from ethanol/water solution). More detailed NMR analyses of compounds **1**, **7**, **8**, **9**, and 6′-*O*-methyl-α-amanitin (**18**)[14] clearly show that these amatoxins assume generally similar conformations in DMSO solution. This study[14] also shows that the conformation of compounds **7** and **8** in DMSO solution compares very well with their corresponding conformation in the crystal (verified again in this paper) and that the conformations of **1** and **18** in DMSO solution correspond well with the conformation of **2** in the crystal. Additionally, the backbone conformation of derivative **10** in the crystal[17] (see also Table V) compares well with the conformation of the corresponding sulfide derivative **18** in DMSO solution.[14]

H/D exchange rates and temperature coefficients measured for the peptide N–H groups of **1**[95] and **7**[14] in DMSO-d_6 also generally correspond to the crystal structures presented above.

(83) Olovsson, I.; Jönsson, P.-G. In *The Hydrogen Bond*; Schuster, P., Zundel, G.; Sandorfy, C., Eds.; North-Holland: Amsterdam, 1976; Vol. II, Chapter 8.
(84) Koetzle, T. F.; Lehmann, M. S., in ref 84a, Vol. II, Chapter 9.
(85) Baker, E. N.; Hubbard, R. E. *Prog. Biophys. Mol. Biol.* **1984**, *44*, 97.
(86) Aubry, A.; Protas, J.; Boussard, G.; Marraud, M.; Neel, J. *Biopolymers* **1978**, *17*, 1693.
(87) Boussard, G.; Marraud, M.; Neel, J. In *Peptides 1976*; Loffet, A., Ed.; Univerity of Brussels: Brussels, 1976; pp 601–607.
(88) Iitaka, Y.; Nakamura, H.; Takada, K.; Takita, T. *Acta Crystallogr.* **1974**, *B30*, 2817.
(89) Bavoso, A.; Benedetti, E.; DiBlasio, B.; Pavone, V.; Pedone, C.; Lorenzi, G. P.; Muri-Valle, V. *Biochem. Biophy. Res. Commun.* **1982**, *107*, 910.
(90) Benedetti, E.; Bavoso, A.; DeBlasio, B.; Pavone, V.; Pedone, C.; Toniolo, C.; Bonora, G. M. *Biochem. Biophys. Res. Commun.* **1983**, *112*, 1056.
(91) Taylor, R.; Kennard, O.; Versichel, W. *J. Am. Chem. Soc.* **1983**, *105*, 5761.
(92) Kollman, P. A. *J. Am. Chem. Soc.* **1972**, *94*, 1837.
(93) Adman, E.; Watenpaugh, K. D.; Jensen, L. H. *Proc. Natl. Acad. Sci., U.S.A.* **1975**, *72*, 4854.
(94) Rosenfield, R. E., Jr.; Parthasarathy, R. *Acta Crystallogr.* **1975**, *B31*, 462.
(95) Tonelli, A. E.; Patel, D. J.; Wieland, Th.; Faulstich, H. *Biopolymers* **1978**, *17*, 1973.

All 5 NH groups involved in intraHB's in the amatoxin structures (Table VIII) exhibit favorable parameters for intramolecular hydrogen bonding in solution. Moreover, the very slow exchange rate of the Gly-5 NH hydrogen (in both **1** and **7**) is probably due to the strong 5→1 intraHB formed by this group in the amatoxins (Table VIII) and due the fact that this NH group is buried within the interior of the molecule[14] (Figures 3 and 4). Similarly, the exchange rate of the Asn-1 NH hydrogen is shown to be significantly slower in **1** than in **7**; this result again corresponds well with the relatively buried location of this group in the structures of **2** and **10**, in comparison to the solvent-accessible location in **7** (Figure 3), and with the bifurcated hydrogen bond observed for this group in **2** and **10** (assuming that the backbone conformation of **1** is similar to those of **2** and **10**, as discussed below). Partial steric shielding of the Ile-6 NH group by the extra OMe group in **7** may contribute to the slower exchange rate measured for this group, and the rotation of the peptide bond might affect the exchange rate of the nearby Cys-8 NH group. Yet, the significantly different exchange rates found for the NH groups of Ile-6 and Cys-8 in **1** and **7**,[14] respectively, cannot be fully accounted for in the related crystal structures. The fast H/D exchange rates of all side chain OH groups and the Asn-1 side chain NH_2 group in **1** further confirm that these groups are not involved in intramolecular interactions and are solvent accessible, as clearly shown by the amatoxin crystal structures (Table IX).

Two recent studies[96,97] of the conformation of two synthetic amatoxin analogues (the D-Ala^5 and the D-Ala^7 derivatives) in solution, using two-dimensional proton NMR techniques, showed that these derivatives adopt practically the same conformation as found for **10** in the crystal structure.

Thus the close relationships between the structures of the amatoxins examined in solution (DMSO) and in the crystal indicate that amatoxin conformations are not affected significantly by crystal-packing forces. The similar CD and ORD spectra of amatoxins in aqueous and organic solvents further indicates that the amatoxin conformations are relatively independent of the polarity of the solvent (the somewhat different CD spectra in DMSO are shown by the NMR studies not to be associated with major conformational changes). Also, the relatively similar structures of amatoxins **2**, **7**, **8**, and **10** in the crystal, despite the different crystallization solvent, the different crystal packing, and the different water content in the unit cell, support the above statements. We therefore conclude that in general an amatoxin molecule would assume the same conformation independently of its surrounding and the medium. This structural independence is probably facilitated by both the bicyclic frame and the strong intramolecular hydrogen bonds in amatoxins which result in a very stable and essentially rigid structure. Similar conformational consistencies, independent of the crystal system and the nature of the crystallization solvent, were indicated for other large cyclic peptides.[61]

Structure–Activity Relationships. Summarizing the structural data presented above, we note the following points that could be of possible relevance to the biological activity of amatoxins: (1) All the amatoxins that have been structurally analyzed in detail (X-ray and NMR) generally exhibit similar overall structure and their conformation in the crystal is very similar to the corresponding conformation in solution. (2) The amatoxin conformations do not seem to be affected significantly by crystal forces and solvent interaction. (3) Five to seven relatively strong intraHB's dominate the conformation of amatoxins, three of which are conserved in all amatoxins now structurally determined. (4) The indole–sulfur transannular covalent bridge is a very stable and rigid unit present in all amatoxins, restricting significantly the number of possible conformations available for the amatoxins molecules. (5) The amatoxin molecules do not experience any significant structural or conformational strain that could have been imposed by the ring closure, the transannular bridge, or the unusual side chains. (6) Points 1–5 indicate that most (if not all) naturally occurring and chemically modified amatoxins probably assume the same basic overall structure shown above and that this structure is probably similar in biological environment (biological fluids, membranes, and inside the cell). (7) Of the functional groups of side chains only the Asn/Asp-1 terminal C=O group and the (*S*)-oxygen on the sulfur participate in intramolecular interactions. When present, the sulfur (*S*)-oxygen forms an intraHB with the NH group of residue 1, thus causing a rotation of ≈90° of the peptide unit between residues 8 and 1. (8) The two OH groups (γ and δ) in the DihyIle-3 side chain, the γ-OH group of HyPro-2, and the (*R*)-oxygen on the sulfur do not affect the overall conformation of amatoxins.

From the above summary it appears that most of the differences in biological activity in amatoxins are likely to be due to differences in chemical nature and local conformations, rather than to major overall conformational changes. For the examination of the possible role of specific groups in the biological activity (transport, penetration, and binding) of amatoxins, all functional groups, including backbone NH and C=O moieties, should be considered. We assume that the NH and C=O groups that participate in intraHB's are less likely to be involved in any other interactions (e.g. binding). Next, we examine the possible role of the remaining functional groups in the amatoxin biological activity on the basis of both the structural data presented above and inhibition and toxicity measurements on different amatoxin derivatives reported in the past.[3,6,7,13]

It is apparent from the data presented in Table I and from similar parameters reported for other amatoxin derivatives that there is no direct correlation between K_i's and LD_{50}'s; that is, inhibition capacity is not completely correlated with toxicity. It was therefore suggested[13] that inhibition of RNA polymerase B activity, although necessary, is not the only factor that determines the toxicity of an amatoxin derivative. Other contributing factors could be those that modulate the effective concentration of the toxin in the cell, namely transport in biological fluids, penetration into the cell and into the nucleous, accumulation in the cell/nucleous, etc. In the following discussion we refer to the capacity to inhibit the enzyme (K_i) as "inhibition" and to the in vivo additional factors as "pharmacokinetics". Biological activity measurements on amatoxins conjugated to macromolecules (see below) demonstrated that the two factors are independent since in most of the cases increased toxicity was detected despite decreased inhibition capacity. It should also be noted that the pharmacokinetic effects are not simply correlated with the overall hydrophobic/hydrophilic character of the amatoxin molecules, suggesting the presence of specific interactions (e.g. a transmembrane carrier) along the pharmacokinetic pathway.

(1) The Asn/Asp-1 terminal NH_2 or OH groups do not participate directly in binding and inhibition since replacement of NH_2 by OH (e.g. 1 vs. 2) makes no difference in either inhibition or toxicity (Table I) and replacement of the OH by OCH_3 or *S*-phenyl groups reduces the toxicity by only a relatively small magnitude.[98,99] Also β-amanitin conjugated to large proteins through the –(C=O)NH– group[3,100,101] exhibits some reduction in inhibitory activity (K_i), but it is relatively insignificant considering the size of these proteins (in fact the toxicity of these conjugates even increases). However, modifications of the –(C=O)NH_2 group to –(C=O)NHR, when R is a large lipophilic group, result in a more significant decrease in toxicity.[98,99] Probably, then, this group is involved in the pharmacokinetics of the amatoxins.

(2) The HyPro-2 γ-OH group probably is directly involved in binding since the lack of this hydroxyl causes about 10^4-fold reduction in the inhibition capacity of amatoxins (e.g. **4** vs **5**). From the crystal structures it looks as if this group can act mainly as a hydrogen donor in an interHB; the acceptor side (lone pairs)

(96) Zanotti, G.; D'Auria, G.; Paolillo, L.; Trivellone, E. *Biochim. Biophys. Acta* **1986**, *870*, 454.
(97) Zanotti, G.; D'Auria, G.; Paolillo, L.; Trivellone, E. In *Proceedings of the 19th European Peptide Symposium*; Porto Carras, Greece, 1986.
(98) Wieland, Th.; Boehringer, W. *Liebigs Ann. Chem.* **1960**, *635*, 178.
(99) Faulstich, H.; Trischmann, H.; Wieland, Th.; Wulf, E. *Biochemistry* **1981**, *20*, 6498.

of the oxygen is directed toward the interior of the molecule and thus may be somewhat protected. As noted above this OH group forms a relatively strong interHB (only as hydrogen donor) in all four amatoxin crystal structures.

(3) The DihyIle-3 δ-OH group is not involved in any biological activity since the lack of this group makes no difference for either inhibition or toxicity (e.g. **1** vs **3**).

(4) The DihyIle-3 γ-OH group may or may not be involved directly in binding to the enzyme since the lack of this group causes only a relatively small reduction in inhibition (e.g. **3** vs **4**). However, this group is probably very important for pharmacokinetics since its absence results in a substantial reduction in toxicity (e.g. **3** vs **4**). As shown in the crystal structures this group is not involved in any intramolecular interaction and is incapable of affecting significantly the overall conformation of the amatoxin molecule. In this view, therefore, the large decrease in the inhibition capacity of aldoamanitin **11** (Table I) is more likely to be, at least in part, a result of an altered binding due to a new amatoxin–enzyme interaction (through the aldehyde group). We cannot exclude, however, the possibility that the reduced inhibition capacity of **11** is due to a local conformational change in the peptide. Preliminary NMR studies on **11** in solution indicate indeed a slight deformation of the backbone of the peptide, yet it is not clear to what extent this slight deformation really alters the binding parameters.[102] Similarly, it is possible, although unlikely, that the γ-OH participates in an important interaction with the enzyme and therefore its absence in **11** is the main cause for the reduced inhibition capacity. In that case, of course, the relatively small reduction in inhibition capacity of amanulin (**4**) should be justified by an alternative explanation (e.g. altered conformation, or altered binding, or both).

(5) The DihyIle-3 β-CH_3 group has been shown to be important for both inhibition and toxicity (e.g. **12** vs **13**). The β-branching is probably essential for a hydrophobic interaction with the enzyme and also determines the local orientation of the γ-OH group.

(6) The HyTrp-4 6′-OH group seems not to be directly involved in either inhibition or pharmacokinetics since the lack of this group (e.g. in **6**) or modification of it to $-OCH_3$ (e.g. in **9**) does not affect either K_i or the LD_{50} (Table I). Moreover, etherification of this hydroxyl with various alkyl groups[7,99] showed generally little effect on the inhibition capacity, and only a relatively small reduction in toxicity for the larger alkyl group.[99] In fact the whole indole moiety seems to be far away from the contact region with the enzyme since conjugation of large proteins and polymers to the indole 6′ and 7′ positions[3,100,101] results in comparatively little reduction in inhibition relative to their size. Also substitution of iodine and alkylamines at either the phenolic 7′ or 5′ positions, or both, showed no decrease in capacity for inhibition.[104,105]

(7) The HyTrp-4 ε-NH group is unlikely to be involved in intermolecular binding (to the enzyme) since *O,N*-dimethyl-α-amanitin exhibits almost full capacity for inhibition.[99]

(8) The Gly-5, Ile-6, Gly-7 bend seems to be at the contact region with the enzyme since substitution of either of them by L-Ala causes substantial reduction in inhibition capacity[13] (Table I). Ile-6 is probably involved with the enzyme in a hydrophobic interaction which is greatly reduced upon substitution to L-Ala. The L-Ala substitutions at the glycine residues can cause a conformational change (local or overall) or steric interference in the binding region of the toxin. A molecular model based on the amatoxin crystal structures suggests that some degree of conformational change is necessary to accommodate the substituted L-Ala, especially in the case of Gly-5 (steric clashing with the close-by indole ring). The model also suggests that substitution of the glycine residues by D-Ala rather than L-Ala is likely to cause less conformational changes (if any). These conformational predictions based on the crystal structure are fully supported by recent NMR studies of these two D-Ala derivatives in solution.[96,97] Furthermore, kinetic studies of the D-Ala[5] and D-Ala[7] amatoxin derivatives indicates significantly less reduction in inhibition capacity of the D-Ala in comparison to the L-Ala derivatives,[96,97] in agreement with the conformational change effect suggested above.

(9) The sulfur group and (*R*)-oxygen seem unlikely to be the involved directly in binding or pharmacokinetics since the biological activities of the (*R*)-sulfoxide and the sulfide derivatives are practically identical (e.g. **1** vs **9**, Table I). The (*S*)-oxygen, however, causes a small (yet significant reduction in inhibition capacity and substantial reduction in toxicity (e.g. **7** vs **9**). The (*S*)-oxygen, when present, forms a strong intraHB with the Asn/Asp-1 NH group and is partially shielded from the exterior by the nearby Asn/Asp-1 side chain and the Trp-4 side chain. In addition, substitutions of rather bulky groups at the close-by (≈3.3 Å) Asn-1 δ-N cause a complete block of the (*S*)-oxygen space but give rise to only a small reduction in biological activity (see above). It is therefore unlikely that the (*S*)-oxygen alters the normal binding mode by forming a new interaction or by steric or polar interference with a group in the binding site. In the same way, the (*R*)-oxygen is not believed to be at the binding site since methyl substitution at the very close (≈2.8 Å) indole ε-NH group affects the inhibition capacity very little (see above). Another proposed explanation for the change in activity based on the difference in the effective polarity of the (*R*)- and (*S*)-sulfoxides and the sulfone[13] also seems unlikely since dipole moments and partial charges are expected to be similar in the three cases, as discussed above. Further, it has been shown that the sulfur group has little effect on the overall conformation of amatoxins,[14] disconfirming the proposed major conformational changes in the (*S*)-sulfoxides.[7,106] Thus it appears that the altered activity in the (*S*)-sulfoxide derivatives[13] is an indirect effect, probably the different position and orientation of the Cys-8 carbonyl group as a result of the rotation of the Cys-8–Asn-1 peptide bond upon hydrogen bonding to the (*S*)-oxygen. Although this carbonyl oxygen atom could be involved slightly in intermolecular binding interaction, it seems to be more critical for pharmacokinetics since the inhibition capacity of **7** is decreased only by ≈8-fold whereas its toxicity is almost completely diminished (**7** vs **9** in Table I). In this view the relatively high biological activity of the sulfone derivative **8**, which also exhibits an altered Cys-8 carbonyl position, could be accounted for, at least in part, by an alternative, yet less favored, interaction with the enzyme through the (*R*)-oxygen as has been suggested previously;[14] this oxygen is close by (≈3.8 Å from the carbonyl oxygen of Cys-8) and points generally in the same direction as the untilted carbonyl group.

The chemical structure–biological activity relationships summarized above, together with the amatoxin crystal structures presented earlier, indicate that the contact of amatoxins with the RNA polymerase enzyme takes place primarily at one side of the amatoxin molecule (side A) whereas the opposite side (side B) seems to be away from the enzyme. Figure 10 presents the assumed binding (A) and nonbinding (B) sides of amatoxins as viewed in a space-filling drawing based on the crystal structure of **8**. Side A is basically the concave side of the 24-membered macrocycle (including HyPro-2 and Ile-6 side chains), and side B is the convex side including the transannular sulfur–indole bridge, Asn-1 side chain, and the terminal (δ)–CH_2OH group of DihyIle-3. The DihyIle-3 γ-OH group, the Cys-8 C=O group, and the sulfur (*R*)-oxygen, being on the edge between these two sides, are likely to contribute only to lesser extent to the binding interaction (and inhibition); however, it seems that these groups form important contact surfaces for pharmacokinetic activity (e.g. interaction with a possible specific transmembrane carrier) which

(100) Cessi, C.; Fiume, L. *Toxicon* **1969**, *6*, 309.
(101) Faulstich, H.; Trischmann, H.; Zobeley, S. In *Amanita Toxins and Poisoning*; Faulstich, H., Kommerell, B.; Wieland, Th., Eds.; Witzstrock: Baden-Baden, 1980; pp 37–42.
(102) Wieland, Th., personal correspondence, 1986.
(103) Faulstich, H.; and Trischmann, H. *Hoppe-Seyler's Z. Physiol. Chem.* **1973**, *354*, 1395.
(104) Morris, P. W.; Venton, D. L.; Kelley, K. M. *Fed. Proc., Fed. Am. Soc. Exp. Biol.* **1977**, *36*, 882 (Abs. 3222).
(105) Morris, P. W.; Venton, D. L.; Kelley, K. M. *Biochemistry* **1978**, *17*, 690.
(106) Buku, A.; Altmann, R.; Wieland, Th. *Liebigs Ann. Chem.* **1974**, 1580.

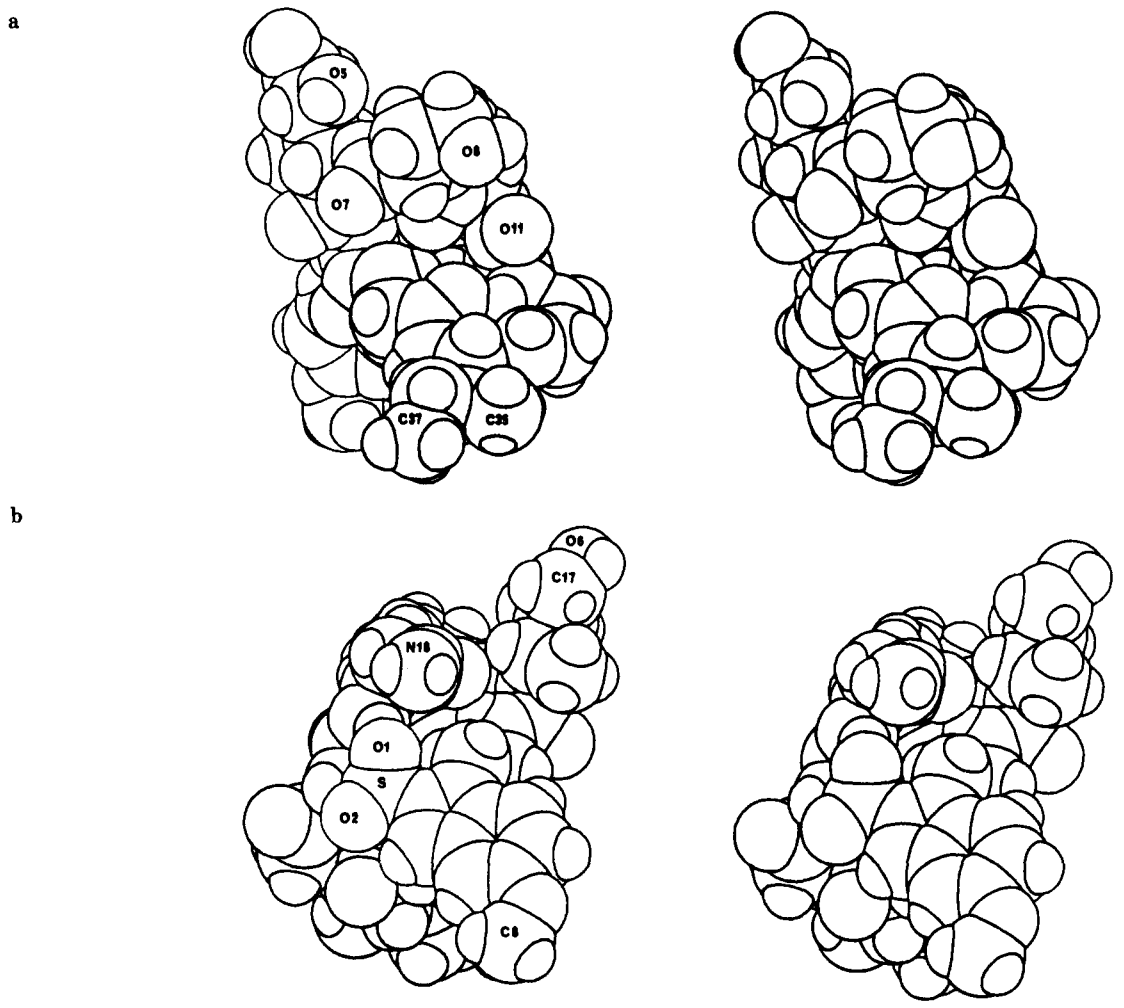

Figure 10. Stereoviews of a space-filling model of 8. (A) A view of the proposed binding surface (side A); (B) a view of the other side of the molecule or the proposed nonbinding surface (side B). Views (A) and (B) are related by a 180° rotation around the vertical axis.

are related, yet different, from the surface interacting with the enzyme. Provided that the amatoxin–RNA polymerase contact is indeed taking place as described above, it it expected that the backbone carbonyl group of HyPro-2, the backbone NH group of Gly-5, and to a lesser extent the backbone carbonyl groups of DihyIle-3 and Gly-7 could participate in binding interaction with the enzyme according to their location on the proposed binding surface (Figure 10). This binding model also indicates that since the Asn/Asp-1 side chain and the sulfur group are not located at the binding surface, the small differences in their local conformations observed in the crystal structures (see above) are insignificant for the biological activity. However, some of the differences in local conformations and orientations of other groups that are located on or near the binding surface (e.g., HyPro-2) could be of functional importance.

On the basis of the model discussed above, it seems as if any kind of blocking (permanent or temporary) of side A of an active amanitin would reduce significantly its binding affinity to the enzyme, thereby reducing its toxicity. It is appealing to assume, therefore, that if one would be able to make monoclonal antibodies specific for side A of an amanitin molecule, it would be possible to use these antibodies for treatment in cases of *Amanita* poisoning. This is assuming, of couse, that the affinity of the toxin to the antibody is similar or greater than its affinity to the enzyme.

Thus it is suggested that the high affinity and strong binding of amanitins to RNA polymerase B is facilitated by the following: (i) a strong hydrogen-bonding interaction through the HyPro-2 γ-OH group (at the center of the proposed binding region), (ii) a strong hydrophobic interaction (e.g. hydrophobic "pocket" in the enzyme binding site) through the Ile-6 side chain, (iii) weaker hydrogen bonding or polar interaction through the DihyIle-3 γ-OH group and Cys-8 carbonyl group, and (iv) possible additional hydrogen-bonding interactions through the backbone NH and C=O groups mentioned above.

It should be emphasized that although the precise overall structure of the amatoxins is shown to be very important for the biological function, the exact role of specific groups and local conformations in the in vitro and in vivo activity of these toxins are only speculative. The proposed explanations for the structure–activity relationships fit generally well most of the experimental observations; however, these should be further evaluated by additional chemical modifications of amatoxins (e.g. hydrophilic substitution in Ile-6 or methylation of the Gly-7 NH group) and would be completely proved (or disproved) only when the actual binding mode of amatoxins with the enzyme is experimentally observed (e.g. in X-ray or NMR analyses of the enzyme–amatoxin complex).

Acknowledgment. We acknowledge the help and encouragement of D. W. Christianson and Drs. D. C. Rees and D. Schomburg in various stages of this work, and we thank Dr. G. Zanotti for helpful discussions and comments. Additionally, we thank the National Institutes of Health (Grant GM06920), and the National Science Foundation (Grant PCM 77-11398) for initial support of the computational laboratory. One of us (G.S.) thanks the Bat-Sheva Function of Israel for a general financial support.

Registry No. 7, 55399-91-2; 7 ($C_{40}H_{56}N_{10}O_{14}S \cdot H_2O \cdot 5.15MeOH$), 120707-40-6; **8**, 55325-99-0; **8** ($C_{40}H_{56}N_{10}O_{15}S \cdot 2.5H_2O \cdot 2.35EtOH$), 120707-41-7; amanitin, 11030-71-0.

Supplementary Material Available: Lists of anisotropic temperature factors for all the non-hydrogen atoms in **7** and **8** (Tables S3 and S4), coordinates and temperature factors of all hydrogen atoms in **7** and **8** (Tables S5 and S6), backbone bond lengths and

bond angles in **7**, **8**, **10**, and **2** (Tables S7 and S8), side chain bond lengths and bond angles in **7**, **8**, **10**, and **2** (Tables S9 and S10), and solvent-solvent interactions in **7** and **8** (Table S11) and stereodiagrams of the extended unit cell packing in **8**, **10**, and **2** (Figures S1, S2, and S3) (12 pages); listing of observed and calculated structure factors for **7** (Table S1) and **8** (Table S2) (59 pages). Ordering information is given on any current masthead page.

σ,π^* Charge-Transfer Excited States of Substituted (Phenylethynyl)pentamethyldisilanes

Keith A. Horn,*,† Robert B. Grossman,‡ Jonathan R. G. Thorne,§ and Anne A. Whitenack†

Contribution from Allied-Signal, Incorporated, Engineered Materials Sector, Morristown, New Jersey 07962, and The University of Pennsylvania, Philadelphia, Pennsylvania 19104. *Received October 17, 1988*

Abstract: A series of substituted (arylethynyl)pentamethyldisilanes was prepared by the palladium(0)-catalyzed coupling of aryl halides and ethynylpentamethyldisilane. The absorption and emission spectra of these acetylenic disilanes were measured over the temperature range from 296 to 77 K in both polar and nonpolar solvents and rigid organic glasses. At 77 K normal $^1(\pi,\pi^*)$ fluorescence and $^3(\pi,\pi^*)$ phosphorescence are observed for those (phenylethynyl)pentamethyldisilanes (**1**) bearing electron-donating substituents (e.g. 4-MeO). At 77 K those (phenylethynyl)pentamethyldisilanes bearing electron-withdrawing substituents (e.g. 4-NC, 4-CO_2Me) show only a unique intramolecular $^1(\sigma,\pi^*)$ charge-transfer (CT) fluorescence in addition to the $^3(\pi,\pi^*)$ state phosphorescence. Neither ground-state CT complex absorption bands nor exciplex emissions were observed in any of the systems studied. The singlet character of these emissive σ,π^* CT states was confirmed by picosecond lifetime measurements. The previously reported photochemical rearrangement of (phenylethynyl)pentamethyldisilanes to silacyclopropenes and silapropadienes as well as the observed photochemical cleavage of (phenylethynyl)pentamethyldisilanes to (phenylethynyl)trimethylsilanes are fully consistent with the σ,π^* CT state assignment. The general involvement of analogous $\sigma\rightarrow\pi^*$ CT or electron transfer in photoexcited polysilanes is suggested by the demonstration of intermolecular fluorescence quenching of electron-deficient benzenes and aryl acetylenes by hexamethyldisilane and dodecamethylcyclohexasilane. The general implications of this type of $\sigma\rightarrow\pi^*$ CT to polysilane photophysics and photochemistry are discussed.

Subsequent to the early reports that the photolysis of alkynyl-substituted disilane derivatives provides a convenient route to silacyclopropene derivatives,[1] photochemical[2] and photophysical[3] investigations have shown that these compounds possess unique singlet intramolecular CT emissive states which dominate their photoreactivities. In the case of (phenylethynyl)pentamethyldisilane (**1a** Y = H, n = 1), the emission spectrum at 77 K in methylcyclohexane/isopentane (MP) was reported to show a normal $^1(\pi,\pi^*)$ fluorescence at 303 nm and a normal $^3(\pi,\pi^*)$ phosphorescence at 410.5 nm. However in addition to these two bands, a third broad, featureless emission band was observed with λ_{max} at 395 nm. This latter emission band was assigned to either a $^1(2p\pi,3d\pi)$ or a $^1(2p\pi,\sigma^*)$ CT state. This band was proposed to originate from a $2p\pi^*$ (aromatic ring) to vacant $3d\pi$ (Si-Si bond) intramolecular charge transfer. The state assignment was based both on the broad, featureless structure of the emission (indicative of a CT state) and by analogy with the broad emission features of photoexcited aryldisilanes which had previously been assigned as singlet $^1(2p\pi,3d\pi)$ CT excited states.[4]

Recent picosecond spectroscopic investigations[5] of alkyl-substituted (phenylethynyl)pentamethyldisilanes have shown that the formation of these CT states occurs very rapidly (<10 ps) both at 77 K and 294 K. It was thus proposed that internal rotation about the acetylene sp hybrid C-Si σ bond is not a prerequisite for formation of the CT states in these molecules and that they are different than other twisted intramolecular charge transfer (TICT) states previously investigated. The rapid formation of these states in rigid organic matrices at 77 K also indicated that solvation changes are not important in the formation of these CT states. On the basis of these spectroscopic investigations, Shizuka and Ishikawa[4] postulated that facile intramolecular CT state formation occurs only in those molecules found in a conformation which places the Si-Si σ bond in the same plane as the phenyl ring. This conformation, it was argued, is the most favorable for $3d\pi$ to $2p\pi$ overlap. Those molecules in the conformation with the Si-Si σ bond out of the plane defined by the phenyl ring would instead only provide efficient overlap of the aromatic π orbitals with the Si-Si σ orbitals.

The decay of the fluorescence of these singlet CT states was reported to have both a fast- and a slow-decay component. For example, (phenylethynyl)pentamethyldisilane (**1a**) showed two

* Author to whom correspondence should be sent: Allied-Signal, Inc., Box 1021R, Morristown, New Jersey 07962.
† Allied-Signal, Inc.
‡ Department of Chemistry, Massachusetts Institute of Technology, Cambridge, Massachusetts 02139.
§ Department of Chemistry, University of Pennsylvania.

(1) (a) Ishikawa, M.; Fuchikama, T.; Kumada, M. *J. Chem. Soc., Chem. Commun.* **1977**, 352. (b) Ishikawa, M.; Fuchikami, T.; Kumada, M. *J. Organomet. Chem.* **1977**, *142*, C45. (c) Ishikawa, M.; Nakagawa, K.; Kumada, M. *Ibid.* **1977**, *131*, C15. (d) Ishikawa, M.; Nishimura, K.; Sugisawa, H.; Kumada, M. *Ibid.* **1980**, *194*, 147.
(2) Ishikawa, M.; Sugisawa, H.; Fuchikami, T.; Kumada, M.; Yamabe, T.; Kawakami, H.; Fukui, K.; Ueki, Y.; Shizuka, H. *J. Am. Chem. Soc.* **1982**, *104*, 2872.
(3) Shizuka, H.; Okazaki, K.; Tanaka, H.; Tanaka, M.; Ishikawa, M.; Sumitani, M.; Yoshihara, K. *J. Phys. Chem.* **1987**, *91*, 2057.
(4) (a) Shizuka, H.; Sato, Y.; Ishikawa, M.; Kumada, M. *J. Chem. Soc., Chem. Commun.* **1982**, 439. (b) Shizuka, H.; Sato, Y.; Ueki, Y.; Ishikawa, M.; Kumada, M. *J. Chem. Soc., Faraday Trans. 1* **1984**, *80*, 341. (c) Shizuka, H.; Obuchi, H.; Ishikawa, M.; Kumada, M. *Ibid.* **1984**, *80*, 383. (d) Hiratsuka, H.; Mori, Y.; Ishikawa, M.; Okazaki, K.; Shizuka, H. *J. Chem. Soc., Faraday Trans. 2* **1985**, *81*, 1665. (e) Shizuka, H.; Okazaki, K.; Tanaka, M.; Ishikawa, M.; Sumitani, M.; Yoshihara, K. *Chem. Phys. Lett.* **1985**, *113*, 89.
(5) (a) Grabowski, Z. R.; Rotkiewski, K.; Siemiarczuk, A.; Cowley, D. J.; Baumann, W. *Nouv. J. Chim.* **1979**, *3*, 443. (b) Grabowski, Z. R.; Dobkowski, J. *Pure Appl. Chem.* **1983**, *55*, 245. (c) Rettig, W. *Angew. Chem., Int. Ed. Engl.* **1986**, *25*, 971.

0002-7863/89/1511-4809$01.50/0